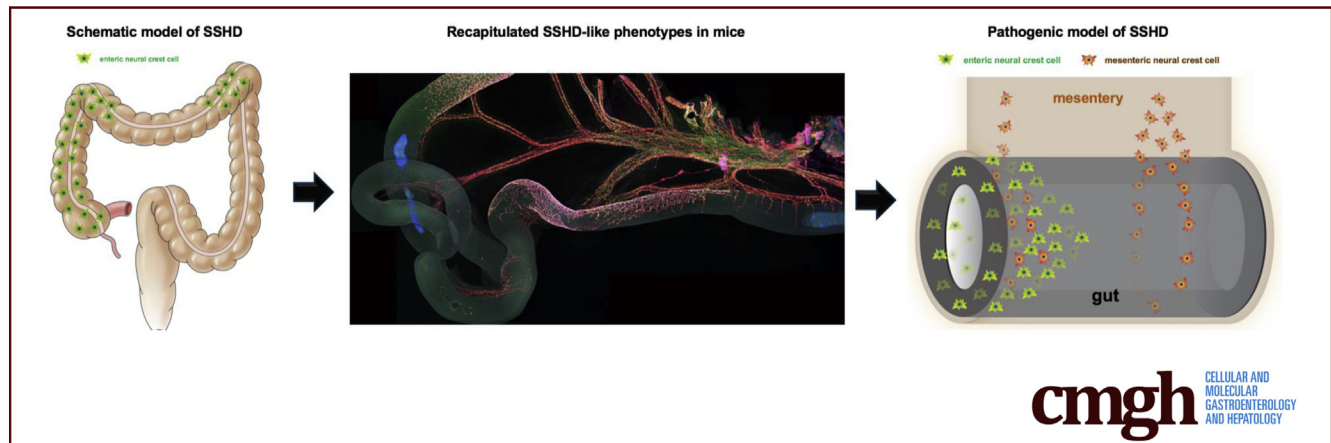# ORIGINAL RESEARCH

Mesenteric Neural Crest Cells Are the Embryological Basis of Skip Segment Hirschsprung's Disease

Qi Yu,[1,*] Mengjie Du,[1,*] Wen Zhang,[2,*] Li Liu,[1] Zhigang Gao,[3] Wei Chen,[4] Yan Gu,[1] Kun Zhu,[5] Xueyuan Niu,[1] Qiming Sun,[6] and Liang Wang[1]

[1]Institute of Neuroscience and Department of Neurology of the Second Affiliated Hospital, National Health Commission and Chinese Academy of Medical Sciences Key Laboratory of Medical Neurobiology, Zhejiang University School of Medicine, Hangzhou, China, [2]Department of Pathology, Wuhan Children's Hospital, Tongji Medical College, Huazhong University of Science & Technology, Wuhan, China, [3]Department of Pediatric General Surgery, The Children's Hospital, Zhejiang University School of Medicine, Hangzhou, China, [4]Institute of Translational Medicine, and Children's Hospital Affiliated and Key Laboratory of Diagnosis and Treatment of Neonatal Diseases of Zhejiang Province, The Children's Hospital, Zhejiang University School of Medicine, National Clinical Research Center for Child Health, Hangzhou, China, [5]Department of Pathology, The Children's Hospital, Zhejiang University School of Medicine, Hangzhou, China, [6]Department of Biochemistry, Department of Cardiology of Second Affiliated Hospital, Zhejiang University School of Medicine, Hangzhou, China

SUMMARY

Mesenteric neural crest cells, a subset of vagal neural crest cells migrating into the gut via the gut mesentery to contribute to the enteric nervous system, are the embryological basis of skip segment Hirschsprung's disease.

BACKGROUND & AIMS: Defective rostrocaudal colonization of the gut by vagal neural crest cells (vNCCs) results in Hirschsprung's disease (HSCR), which is characterized by aganglionosis in variable lengths of the distal bowel. Skip segment Hirschsprung's disease (SSHD), referring to a ganglionated segment within an otherwise aganglionic intestine, contradicts HSCR pathogenesis and underscores a significant gap in our understanding of the development of the enteric nervous system. Here, we aimed to identify the embryonic origin of the ganglionic segments in SSHD.

METHODS: Intestinal biopsy specimens from HSCR patients were prepared via the Swiss-roll technique to search for SSHD cases. NCC migration from the neural tube to the gut was spatiotemporally traced using targeted cell lineages and gene manipulation in mice.

RESULTS: After invading the mesentery surrounding the foregut, vNCCs separated into 2 populations: mesenteric NCCs (mNCCs) proceeded to migrate along the mesentery, whereas enteric NCCs invaded the foregut to migrate along the gut. mNCCs not only produced neurons and glia within the gut mesentery, but also continuously complemented the enteric NCC pool. Two new cases of SSHD were identified from 183 HSCR patients, and *Ednrb*-mutant mice, but not *Ret*^{-/-} mice, showed a high incidence rate of SSHD-like phenotypes.

CONCLUSIONS: mNCCs, a subset of vNCCs that migrate into the gut via the gut mesentery to give rise to enteric neurons, could provide an embryologic explanation for SSHD. These findings lead to novel insights into the development of the enteric nervous system and the etiology of HSCR. *(Cell Mol Gastroenterol Hepatol 2021;12:∎–∎; https://doi.org/10.1016/j.jcmgh.2020.12.010)*

The enteric nervous system (ENS), the intrinsic nervous system of the gut that regulates the movement, blood flow, and secretion of the gastrointestinal (GI) tract, is derived

primarily from vagal neural crest cells (vNCCs), which arise at the level of somites 1–7, invade the foregut, and rostrocaudally colonize the gut.[1,2] According to current dogma, Hirschsprung's disease (HSCR), a congenital ENS disorder characterized by aganglionosis in variable lengths of the distal intestine, is caused by the incomplete colonization of the gut by vNCCs.[3,4] However, the occurrence of skip segment Hirschsprung's disease (SSHD), a rare variant of HSCR involving a "skip area" of ganglion cell containing intestine within an otherwise aganglionic intestine, contradicts the current consensus about the pathogenesis of HSCR, and lacks a clear embryologic basis.[5] Furthermore, given that the histologic evaluation of a rectal suction biopsy is the gold standard for HSCR diagnosis,[6] the presence of a skip area in the distal rectum of SSHD patients consequently might lead to a false-negative diagnosis.[7] Therefore, the characterization of the embryonic origin of the segmental ENS in SSHD not only will further our understanding of ENS development, but also will support the development of potential HSCR treatments.

Since the first case of SSHD was reported in 1954,[8] 34 SSHD cases have been reported, with skip segments occurring from the ileum to the rectum (Table 1).[7,9-30] In addition to vNCCs, sacral NCCs (sNCCs) also generate the colonic ENS in mice and chickens,[31,32] and these cells thus have been proposed as the source of segmental ENS in SSHD. However, this hypothesis cannot explain the occurrence of most skip segments within the proximal colon. Moreover, the invariable aganglionosis of the distal bowel in HSCR patients is inconsistent with the contribution of sNCCs to the colonic ENS in human beings.[3] Alternatively, the skip area might be caused by neuroblasts, which emanate from the bowel wall at the ileocecal junction, migrate along the mesenteric border, and reinvade the colon.[33,34] Consistent with this theory, a recent study showed that trans-mesenteric NCCs (tmNCCs), a population of midgut enteric NCCs (eNCCs) that migrate via the mesentery into the hindgut, are the main source of the colonic ENS.[35] Thus, the skip area in the hindgut could be logically explained as a failure of neuroblasts or tmNCCs to merge with delayed eNCCs from the foregut.[36,37] Notwithstanding, neuroblasts or tmNCCs theory cannot provide a convincing explanation for the presence of ganglionic segments within otherwise aganglionic small intestine and cecum. In lampreys and mice, Schwann cell precursors (SCPs) have been shown to invade the gut along extrinsic axons to give rise to a population of enteric neurons,[37,38] subsequently leading to the speculation that SCPs might be the potential source of the segmental ENS. Given that one distinguishing characteristic of SCPs is their intimate association with extrinsic axons,[39] the patterns of SCP-derived segmental ENS should be expected to be consistent with the innervation pattern of extrinsic axons within the aganglionic gut. By contrast, pathologic studies have shown hypertrophic extrinsic innervation in most aganglionic guts from HSCR patients and HSCR animal models.[40,41] Therefore, the SCP hypothesis could not provide a convincing explanation for the distinctive patterns between segmental ENS and extrinsic axons within the aganglionic gut. Moreover, although a recent study showed that up to 20% of colonic enteric neurons are of SCP origin,[37] segmental ENS rarely are detected within the aganglionic gut of HSCR patients, thus suggesting that SCPs are less likely to be the origin of segmental ENS.

The mesentery, which surrounds the entire GI tract to provide a conduit for nerves and blood vessels to the intestine, recently was classified as an individual organ.[42] Previous studies have identified NCCs within the mesentery of HSCR murine models,[33,43] indicating that the mesentery might serve as a migratory route by which NCCs traverse the whole gut. Here, we addressed this hypothesis in mice, using targeted genetic cell tracing and gene manipulation. We showed that a subset of vNCCs delaminate from the neural tube, migrate caudally along the mesentery, and invade the whole gut to make a continuous complementary contribution to the eNCC pool. *Ednrb*-deficient mice, in which vNCCs preferentially migrate through the gut mesentery—rather than along the less-permissive gut—to form innervated skip segments within the aganglionic intestine, recapitulate the phenotypes of SSHD. Together with the 2 new SSHD cases identified from 183 HSCR patients, our study indicates that mesenteric NCCs are the embryologic basis of SSHD.

Results

NCCs Migrate Into the Gut Mesentery to Give Rise to Neurons and Glia

Because previous observations have indicated that tmNCCs emanate from the midgut, cross the mesentery, and invade the hindgut between embryonic day (E) 11.5 and E12.5,[35] we first investigated whether NCCs were present within the mesentery after E12.5, once tmNCC migration had ceased. Given that SCPs are distinguished from NCCs by their intimate association with axons, we performed the general axon marker neuron-specific class III beta-tubulin (TUJ1) staining of the GI tract of NCC-specific $Wnt1^{Cre};R26^{tdTom}$ mouse embryos to distinguish axon-associated SCPs from freely migrating NCCs within the gut mesentery. Many axon-unassociated tandem dimer tomato (tdTom)-expression cells (hereinafter referred to as $Wnt1^{TOM+}$ cells) were scattered in the gut mesentery of $Wnt1^{Cre};R26^{tdTom}$ embryos at E12.5, and rapidly increased in

Most current article

Table 1. Cases of SSHD Reported in the Literature Since 1954

| Reference	Year	Sex	Patients, n	Location of skip segment
Keefer[8]	1954	M	1	Rectosigmoid with skip in sigmoid
Sprinz[9]	1961	F	1	TCA except skip in transverse colon
MacIver[10]	1972	M	1	Rectosigmoid with skip in sigmoid
Martin[11]	1979	M	1	TCA except skip in transverse colon
De Chadarevian[12]	1982	M	1	TCA except skip in transverse colon
Yunis[13]	1983	M	5	TCA except skip in transverse colon
		M		TCA except skip in transverse colon
		M		TCA except skip in transverse colon
		M		TCA except skip in transverse colon
		M		TCA except skip in ascending colon
Taguchi[14]	1983	M	1	TCA except skip in ascending colon
Seldenrijk[15]	1986	M	2	TCA with multiple skips
		F		TCA with multiple skips
Anderson[16]	1986	M	1	TCA except skip in ascending colon
Kapur[17]	1995	F	3	TCA except skip in ascending colon
		F		TCA except skip in cecum
		F		TCA except skip in ascending colon
Yang[18]	2005	M	3	TCA with multiple skips
		M		TCA with multiple skips
		M		TCA with multiple skips
Ziad[19]	2006	M	2	TCA except skip in transverse colon
		F		TCA except skip in cecum
Oshio[20]	2008	M	1	TCA except skip in ascending colon
O'Donnell[21]	2010	M	1	TCA with skip in transverse colon
Doi[22]	2011	F	1	TCA with skip in transverse colon
Burjonrappa[23]	2012	M	1	TCA except skip in ascending colon
Moore[24]	2013	M	2	Skip in right and descending colon
		F		Skip in ascending colon and appendix
Erten[25]	2014	M	1	TCA except skip in hepatic flexure
Raghunath[26]	2014	M	1	TCA with skip in ascending colon and hepatic flexure
Gross[27]	2015	M	1	Skip in transverse and descending colon
Ruiz[28]	2016	M	1	TCA except skip in cecum and ascending colon
Coe[7]	2016	M	2	Skip in the distal rectum
		M		Skip in the distal rectum
Alfawaz[29]	2017	M	1	Skip in proximal sigmoid
Shenoy[30]	2019	M	1	Skip in anal verge
Current cases	2021	M	2	Rectosigmoid with skip in sigmoid
		M		Skip in the transverse colon

numbers at E13.5 and E14.5 (Figure 1*A* and *B*). These mesenteric $Wnt1^{TOM+}$ cells expressed specific NCC markers, including NESTIN, sex determining region Y-box10 (SOX10), paired-like homeobox 2b (PHOX2B), pan-neurotrophin receptor P75NTR (P75), ret proto-oncogene (RET), and human epidermal growth factor receptor 3 (ERBB3), but neither a canonical pericyte marker neuron-glial antigen 2 (NG2) nor a blood epithelial cell marker platelet and endothelial cell adhesion molecule 1 (PECAM-1) (Figure 1*C* and *D*). Moreover, the proliferative capacity of these mesenteric $Wnt1^{TOM+}$ cells was similar to that of pre-enteric NCCs (Figure 1*E* and *F*). To examine whether these freely migrating $Wnt1^{TOM+}$ cells could give rise to neurons and

glia, we tested the GI tract from E14.5 $Wnt1^{Cre};R26^{tdTom}$ mouse embryos for TUJ1 and brain fatty acid-binding protein (B-FABP) expression: these proteins are specific markers for neurons and glia, respectively. As expected, scattered $TOM^{+}/TUJ1^{+}/B$-FABP^{-} and $TOM^{+}/TUJ1^{-}/B$-FABP^{+} cells were observed simultaneously within the gut mesentery, showing that mesenteric $Wnt1^{TOM+}$ cells differentiated into both neurons and glia (Figure 2*A* and *B*). Because these results showed that mesenteric $Wnt1^{TOM+}$ cells possessed all of the distinct characteristics of NCCs, we refer to these cells hereafter as mesenteric NCCs (mNCCs).

To further examine whether mNCCs could generate different neuronal subtypes, we traced mNCC-derived

neurons by crossing $Phox2b^{FLP};R26^{FLTG}$ mice with various neuron-specific Cre mouse lines (hereinafter referred to as $Neuron^{Cre}$ lines). In these $Phox2b^{FLP};Neuron^{Cre};R26^{FLTG}$ mice, NCC-derived neurons ($Phox2b^+$/neuron$^+$) were labeled with green fluorescent protein (GFP) through flippase (FLP)-flippase recognition target (FRT) and Cre-loxp (locus of X-over P1) double recombination (Figure 2C).[44,45] At E14.5, many $Chat^{GFP+}$, Dbh^{GFP+}, and Vip^{GFP+} neurons, as well as scattered $vGat^{GFP+}$ neurons, were detected within the gut mesentery of various $Phox2b^{FLP};Neuron^{Cre};R26^{FLTG}$ embryos (Figure 2D and E), indicating that mNCCs
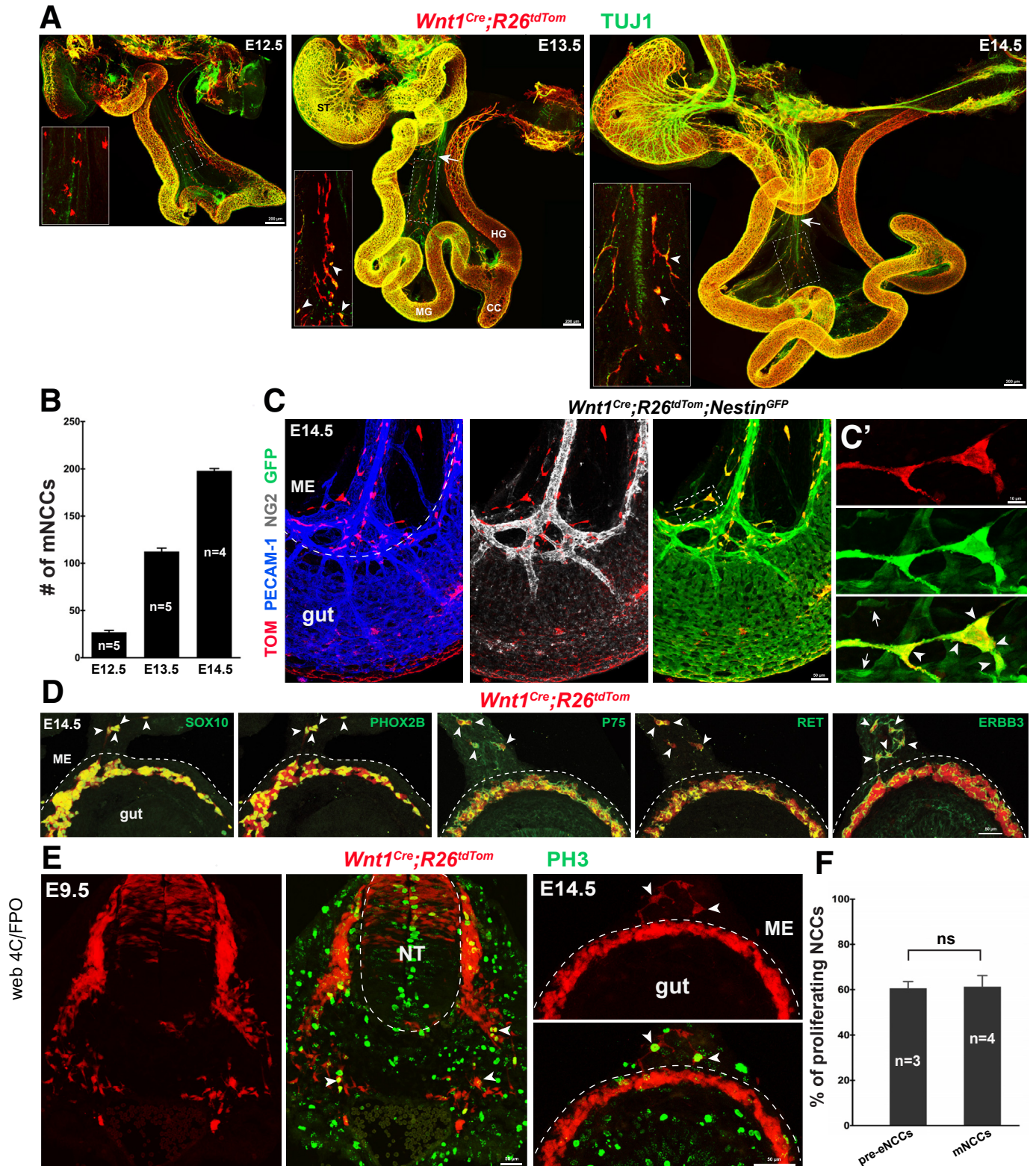
differentiated into distinctive types of mesenteric neurons. Notably, mNCC-derived cholinergic ($Chat^{GFP+}$) and noradrenergic (Dbh^{GFP+}) neurons persisted in the gut mesentery of postnatal $Phox2b^{FLP};Neuron^{Cre};R26^{FLTG}$ mice (Figure 2F).

Collectively, our results showed that some NCCs migrated into the gut mesentery to give rise to mesenteric neurons and glia during embryonic development.

mNCCs Are a Subpopulation of vNCCs That Migrate Directly From the Neural Tube Into the Mesentery

Next, we sought to identify the embryonic origin of mNCCs. Based on their distribution patterns within the gut mesentery between E12.5 and E14.5 (Figure 1A), mNCCs might be either a subpopulation of vNCCs that instead of invading the foregut migrate directly into the mesentery or, alternatively, residual actively proliferating tmNCCs within the gut mesentery. To distinguish between these 2 possibilities, we first spatiotemporally traced vNCCs between E9.0 and E11.5, the stages that encompass the migration of vNCCs from the neural tube to the midgut.[46] Contrary to current consensus, which suggests that vNCCs invade the foregut at E9.5,[47] our tracing experiments showed the presence of many vNCCs within the mesentery of $Wnt1^{Cre};R26^{tdTom}$ embryos at E10.5 and E11.5 (Figure 3). Meanwhile, we noticed that both trunk NCCs and sacral NCCs did not express PHOX2B (Figure 3, top panel), thus indicating that PHOX2B$^+$ mNCCs were a population of vNCCs. Therefore, some vNCCs seemed to migrate directly into the gut mesentery during early development.

Previous observations have indicated that SCPs are guided into the esophagus and stomach by vagus nerves to produce enteric neurons.[48] To test whether the earlier-identified mesenteric vNCCs might represent axon-associated SCPs, we selectively traced nodose ganglion-arising pioneer vagus sensory axons with the $vGlut2^{Cre};R26^{tdTom}$ reporter mouse line.[49] We also performed PHOX2B and TUJ1 immunodetection to simultaneously visualize vagus axons (TOM$^+$/TUJ$^+$), enteric neurons (TOM$^-$/TUJ$^+$), vNCCs (TOM$^-$/PHOX2B$^+$/TUJ1$^-$), and axon-associated SCPs (TOM$^-$/PHOX2B$^+$/TUJ1$^-$) (Figure 4A). At E10.5, vagus axons projected mainly along the ventral mesenchyme adjacent to the esophagus. By contrast, vNCCs migrated far ahead of pioneer vagus axons, and the front of migrating NCCs had reached the midgut

(Figure 4A'). Meanwhile, plenty of TOM$^-$/PHOX2B$^+$/TUJ1$^-$ axon-unassociated vNCCs were present within the mesentery adjacent to the gut (Figure 4A'). To obtain further evidence for this observation, consecutive sections of E10.5 $vGlut2^{Cre};R26^{tdTom}$ embryos were collected to examine the distribution of vNCCs. vNCCs were detected within the dorsal mesenchyme adjacent to the esophagus, stomach, and duodenum. These vNCCs in the mesentery were well positioned to migrate into the bowel, consistent with the dorsal to ventral gradient distribution of eNCCs within the E10.5 gut (Figure 4B–E). Thus, we concluded that mNCCs are a subset of vNCCs that migrate directly into the mesentery.

mNCCs and tmNCCs Might Be the Same Population of vNCCs

The earlier-described finding that some vNCCs migrate directly into the mesentery suggested that tmNCCs, which putatively arise from eNCCs in the midgut, might actually be the same population of mNCCs. To gain evidence for this speculation, we first performed whole-mount staining of the $vGlut2^{Cre};R26^{tdTom}$ mouse gut at E11.5 when the midgut and hindgut were closely opposed to allow the transmesenteric crossing of tmNCCs. We found that a narrow stream of vNCCs were distributing along the gut–mesentery boundary (Figure 5A). Analysis of consecutive sections further showed the presence of vNCCs in the mesentery surrounding the esophagus, stomach, and duodenum, thus suggesting that so-called tmNCCs likely were descending vNCCs (Figure 5B–D). Because previous studies have not provided direct evidence showing the site of tmNCC origin,[35] and because the intimate association between the mesentery and the gut wall made it extremely challenging to determine the origination site of tmNCCs, we used an alternative investigation strategy. That is, we traced the migration of tmNCCs within the gut of $Ednrb^{-/-}$ embryos, a mouse model of HSCR in which the migration of eNCCs along the gut is severely delayed.[50] If tmNCCs truly arise from eNCCs, the absence of midgut eNCCs should induce a concomitant absence of tmNCCs within the mesentery. At E11.5 in the severely affected $Wnt1^{Cre};R26^{tdTom};Ednrb^{-/-}$ embryos, some NCCs remained within the mesentery surrounding the eNCC-absent stomach, and also within the gut mesentery between the midgut and hindgut (Figure 5E and E'). Given that eNCCs migrated along the developing gut in

---

Figure 1. (*See previous page*). **Mesenteric $Wnt1^{TOM+}$ cells possess distinct characteristics of NCCs.** (A) Whole-mount TUJ1 staining of gut preparations from E12.5, E13.5, and E14.5 $Wnt1^{Cre};R26^{tdTom}$ embryos. *Insets* are magnified view of the corresponding *boxed regions*. *Arrows* and *arrowheads* indicate pioneer extrinsic axons and mNCC-derived neurons (TOM$^+$/TUJ1$^+$), respectively. (B) Quantification of the number of mNCCs within the entire gut mesentery (n indicates the number of samples). (C) Representative midgut segment of E14.5 $Wnt1^{Cre};R26^{tdTom};Nestin^{GFP}$ embryos showing colocalization of TOM with GFP, but not with NG2 or PECAM-1. (C') Magnification of the boxed area in C. *Arrows* and *arrowheads* indicate TOM$^-$/GFP$^+$ and TOM$^+$/GFP$^+$ cells, respectively. (D) Transverse sections of an E14.5 $Wnt1^{Cre};R26^{tdTom}$ midgut showing colocalization of TOM with indicated antibodies (*arrowheads*) within the gut mesentery. (E) PH3 staining of transverse sections from an E9.5 embryo and an E14.5 midgut. *Arrowheads* indicate proliferating NCCs. *Dashed curve lines* (C, D, and E) indicate the gut-mesentery boundary. (F) Quantification of the percentages of proliferating pre-enteric NCCs (pre-eNCCs) and mNCCs (n indicates the number of samples; $P = .654$). Serial sections of 60-μm thickness at the level of somites 1–7 from E9.5 embryos were collected for quantification. Ten midgut sections of 60-μm thickness from E14.5 embryos were collected randomly for quantification. CC, cecum; HG, hindgut; ME, mesentery; MG, midgut; NT, neural tube; ST, stomach.
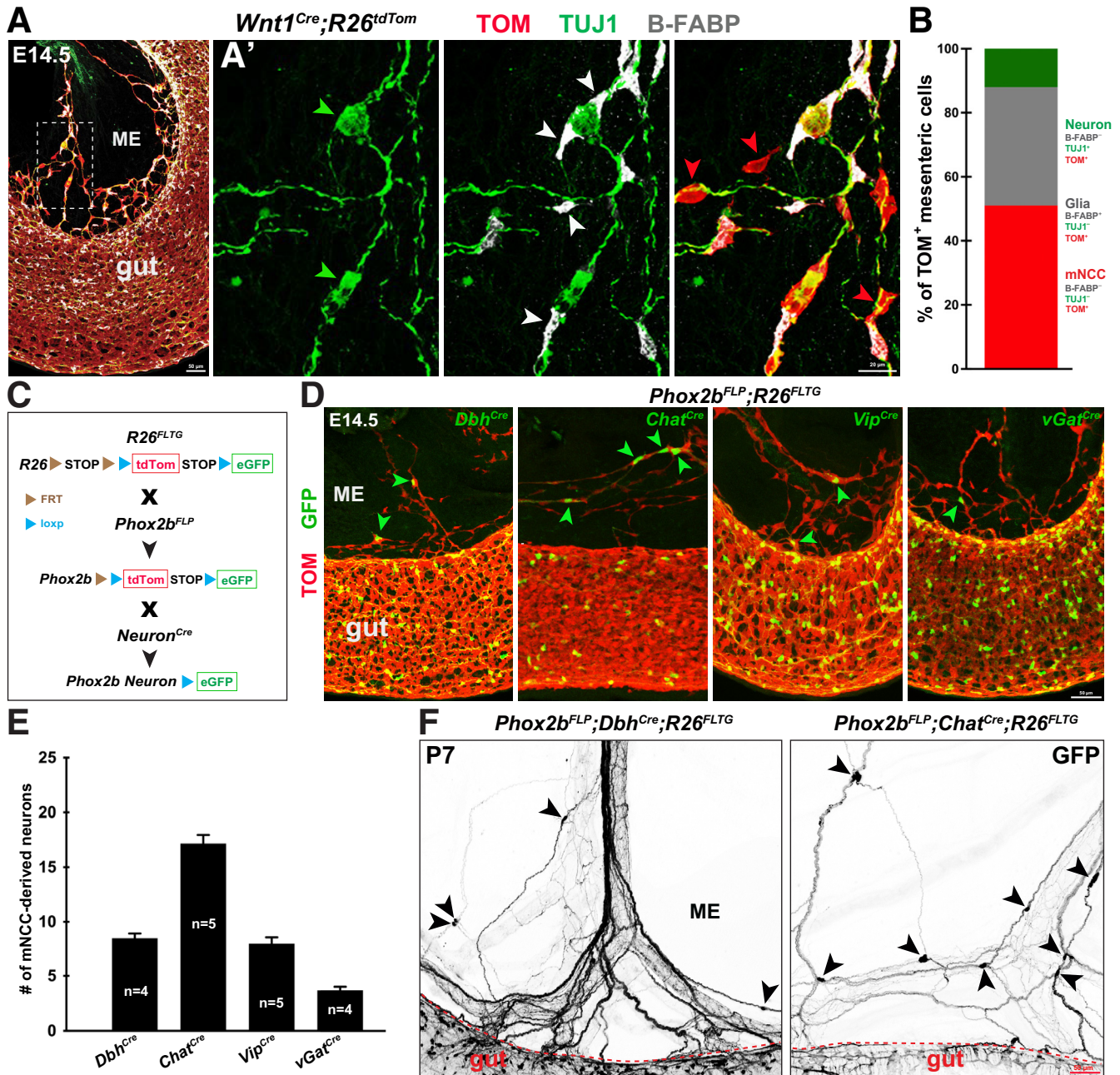
Figure 2. mNCCs give rise to neurons and glia within the gut mesentery. (*A*) Representative midgut segment from E14.5 *Wnt1^Cre^;R26^tdTom^* embryos with B-FABP and TUJ1 staining. (*A'*) Magnified view of the *boxed area* in panel *A* showing mNCC-derived neurons (*green arrowheads*), mNCC-derived glia (*white arrowheads*), and mNCCs (*red arrowheads*). (*B*) Relative proportions of mNCCs, NCC-derived neurons, and NCC-derived glia within the E14.5 gut mesentery (n = 1026 mNCCs from 5 embryos). (*C*) Schematic illustration of the generation of *Phox2b^FLP^;Neuron^Cre^;R26^FLTG^* transgenic mice. (*D*) Genetic tracing of mNCC-derived *Dbh^GFP+^*, *Chat^GFP+^*, *Vip^GFP+^*, and *vGat^GFP+^* neurons (*arrowheads*). Note the presence of eNCC-derived *Dbh^GFP+^*, *Chat^GFP+^*, *Vip^GFP+^*, and *vGat^GFP+^* neurons within the gut. (*E*) Quantification of the number of mNCC-derived neurons within the gut mesentery between the midgut and hindgut of E14.5 embryos (n indicates the number of samples). (*F*) Representative midgut segments from P7 *Phox2b^FLP^;Dbh^Cre^;R26^FLTG^* and *Phox2b^FLP^;Chat^Cre^;R26^FLTG^* mice. *Arrowheads* indicate mNCC-derived *Dbh^GFP+^* and *Chat^GFP+^* mesenteric neurons. FRT, flippase recognition target; ME, mesentery.

chain-like arrays, the skip NCCs in the duodenum of E11.5 *Ednrb^-/-^* embryos likely were derived from mNCCs (Figure 5*E* and *E'*). At E12.0, many mNCCs were adjacent to the eNCC-absent midgut (Figure 5*F* and *F'*). Consistent with the hypothesis that these mNCCs migrate into the bowel, tissue sections showed NCCs both in the mesentery and in

the bowel adjacent to mesentery, but not at the anti-mesenteric margin (Figure 5*F''*). Therefore, the absence of eNCCs within the midgut did not result in the elimination of NCCs within the mesentery, thus strongly suggesting that mNCCs and tmNCCs might be the same population of descending vNCCs.
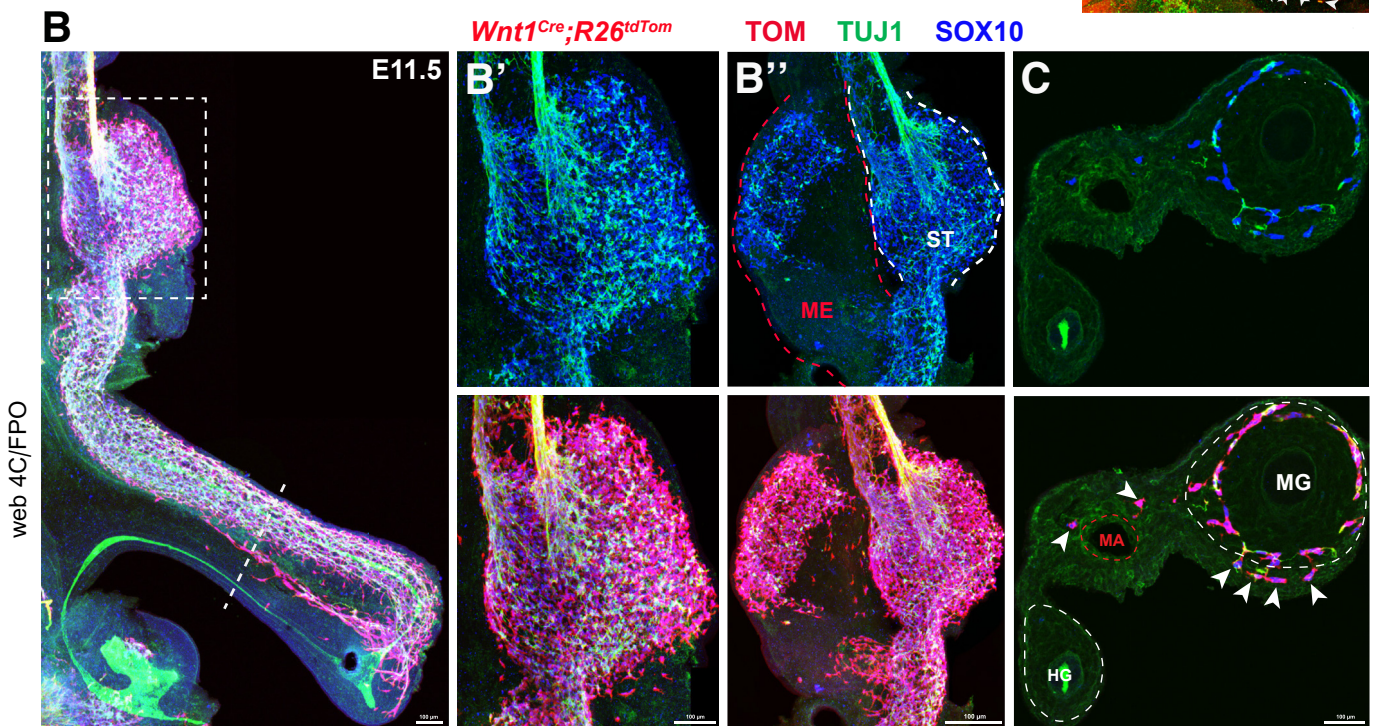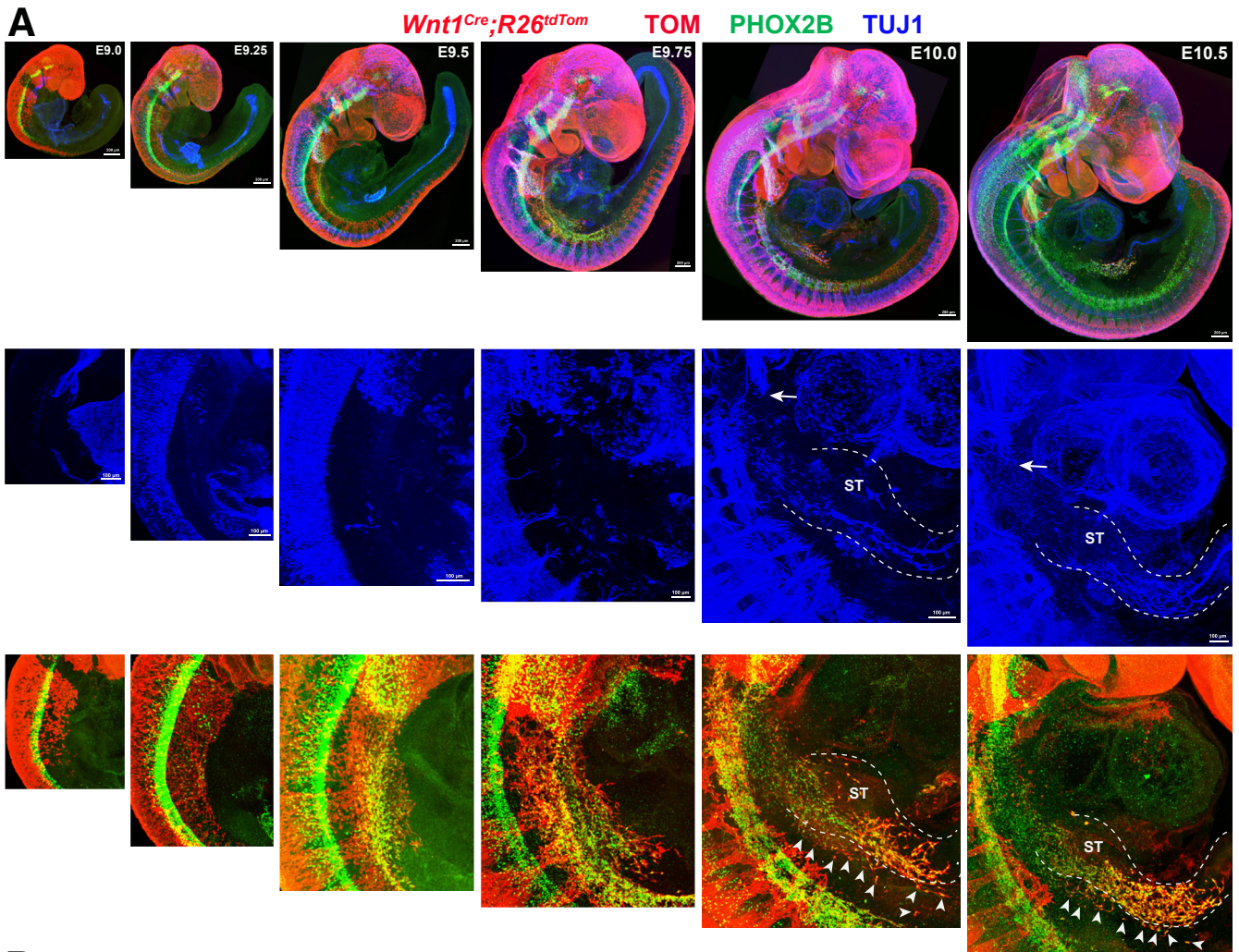
mNCCs Migrate Into the Gut to Contribute to the ENS

We proceeded to investigate whether mNCCs could give rise to enteric neurons. Because of the lack of specific markers that distinguish mNCCs from eNCCs, we first used the difference in the developmental stages of mNCCs and eNCCs at E14.5. At this point, the majority of eNCCs have differentiated into neurons,[51] whereas most mNCCs maintain the undifferentiated state. Therefore, we aimed to temporally trace mNCCs at E14.5 with the NCC-specific cre recombinase-mutated estrogen receptor (CreERT) mouse line by injecting tamoxifen (TM) at E14.0. With this strategy, mNCCs and their derivatives, but not the enteric neurons that arose before TM treatment, would be genetically labelled, thus allowing us to trace their migration into the gut. Rapid silencing of wnt family member 1 (Wnt1) activity in NCCs after their delamination from the neural tube excluded the possibility to temporally trace mNCCs with the $Wnt1^{CreERT}$ mouse line.[52] Although the $Plp1^{CreERT2};R26^{tdTom}$ mouse line has been widely used for temporal lineage tracing of SCPs, recent studies have shown that TM treatment at E9.5 resulted in prominent labeling of NCCs,[53] indicating that the $Plp1^{CreERT2}$ line could be used for genetic fate mapping of NCCs. In agreement with this speculation, TM-induced recombination at E7.5 $Plp1^{CreERT2};R26^{tdTom}$ embryos resulted in the specific expression of TOM in both premigratory and migratory NCCs at E9.5 (Figure 6A). In addition, lineage tracing in $Plp1^{CreERT2};R26^{tdTom}$ embryos activated by injecting TM at E9.0, the stage when most NCCs have left the neural tube, similarly showed that TOM was expressed by the majority of both mNCCs and eNCCs at E14.5 (Figure 6C and E). Thus, inducible Cre activity in the $Plp1^{CreERT2};R26^{tdTom}$ embryos allowed us to temporally trace both premigratory and migratory NCCs.

In $Plp1^{CreERT2};R26^{tdTom}$ embryos, as expected, after the induction of recombination at E14.0 by TM administration, harvesting at E14.5 yielded a significantly higher percentage of traced mNCCs than that of eNCCs. Meanwhile, we found that $Plp1^{TOM+}$ mNCCs formed streams to migrate into the midgut, leading to the accumulation of traced cells along the mesenteric wall (Figure 6D and E). We next examined whether mNCCs could give rise to enteric neurons. Because cholinergic neurons are the most abundant neurons in the ENS,[54] we crossed $Plp1^{CreERT2};R26^{tdTom}$ mice with the $Chat^{GFP}$ cholinergic neuron reporter line, and activated genetic recombination by TM injection at E14.0. After 12 hours of tracing, both cholinergic (TOM$^+$/GFP$^+$/SOX10$^-$) and noncholinergic (TOM$^+$/GFP$^-$/SOX10$^-$) neurons were detected within the midgut of the $Plp1^{CreERT2};R26^{tdTom};Chat^{GFP}$ embryos (Figure 6F and G). Based on the distribution pattern of $Plp1^{TOM+}$ cells within the gut, together with the distinctive recombination efficiency between mNCCs and eNCCs in $Plp1^{CreERT2}$ mice, these traced enteric neurons most likely were derived from mNCCs.

To directly visualize the mesentery–gut migration of mNCCs, we further traced mNCCs in $Wnt1^{Cre};R26^{tdTom};Ednrb^{-/-}$ mouse embryos. In these embryos, the $Ednrb$ knockout severely delays eNCC migration, thus allowing us to follow the migration of mNCCs into an eNCC-absent gut. At E13.5, in contrast to the wild-type embryos, in which the eNCCs migrated rostrocaudally in chains and formed a meshwork of cell strands along the gut (Figure 7A), $Ednrb^{-/-}$ eNCCs were more dispersed and the integrity of the enteric meshwork was severely disrupted. Scattered independent clumps of NCCs were observed distributed along the foregut and midgut (Figure 7B and B''). Occasionally, we observed single cells extending from the mesentery to the bowel wall (Figure 7B'), consistent with the hypothesis that some cells transition between mesentery and bowel wall. These observations suggested that the gut of $Ednrb^{-/-}$ embryos was not colonized by eNCCs in a rostral-to-caudal manner, but by mNCCs in a mesenteric-to-antimesenteric manner. As embryonic development proceeded to E14.5, mNCCs formed a segmental enteric network in the aganglionic gut (Figure 7C). Co-detection of B-FABP and TUJ1 indicated that mNCCs differentiated into both enteric neurons and glia (Figure 7C' and C''). With the development of the segmental ENS, comparable normal enteric meshwork was detected within the aganglionic gut of E15.5 $Wnt1^{Cre};R26^{tdTom};Ednrb^{-/-}$ embryos (Figure 7D). Simultaneously, SCPs (TOM$^+$/B-FABP$^+$) were associated intimately with, but lagged behind, extrinsic axons within the aganglionic gut, and no independent NCCs were observed in the vicinity of pelvic ganglion-arising nerve terminals (Figure 7D'), thus ruling out the potential possibility that the observed segmental ENS was derived from sNCCs or SCPs.

Collectively, these results strongly indicated that mNCCs continuously undergo mesentery–gut migration to enlarge the eNCC pool.

mNCCs Are the Embryonic Origin of the Segmental ENS in SSHD

Our finding that a subset of vNCCs migrated via the gut mesentery to give rise to enteric neurons prompted us to

---

Figure 3. (*See previous page*). **Some vNCCs migrate along the mesentery during early developmental stages.** (*A*) *Top panel*: Whole-mount images of $Wnt1^{Cre};R26^{tdTom}$ embryos with PHOX2B and TUJ1 staining showing the migration of vNCCs from E9.0 to E10.5. Note that PHOX2B is expressed in vNCCs and sympathetic neurons, but not in trunk NCCs or sacral NCCs. *Middle panel*: Magnified views of the corresponding regions from the *top panels* with TUJ1 staining. *Bottom panel*: Same regions as in the *middle panel* with TOM and PHOX2B staining. Based on TUJ1 signal, the presumptive margins of the gut are indicated by *dotted lines*. *Arrowheads* indicate vNCCs within the mesentery, and *arrows* indicate pioneer vagus axons. (*B*) Whole-mount image of an E11.5 gut. The *dotted line* marks the site of the transverse section in panel *C*. (*B'*) Magnified view of the *boxed area* in panel *B*. (*B''*) Whole-mount image of an E11.5 gut, in which the gut mesentery and the stomach are separated. Note the presence of NCCs and NCC-derived neurons (TUJ1$^+$) within the gut mesentery. (*C*) Transverse section through the midgut and hindgut. *Arrowheads* indicate mNCCs within the gut mesentery. *White dotted lines* mark presumptive margins of the midgut and hindgut. *Red dotted line* marks the mesenteric artery. HG, hindgut; MA, mesenteric artery; ME, mesentery; MG, midgut; ST, stomach.
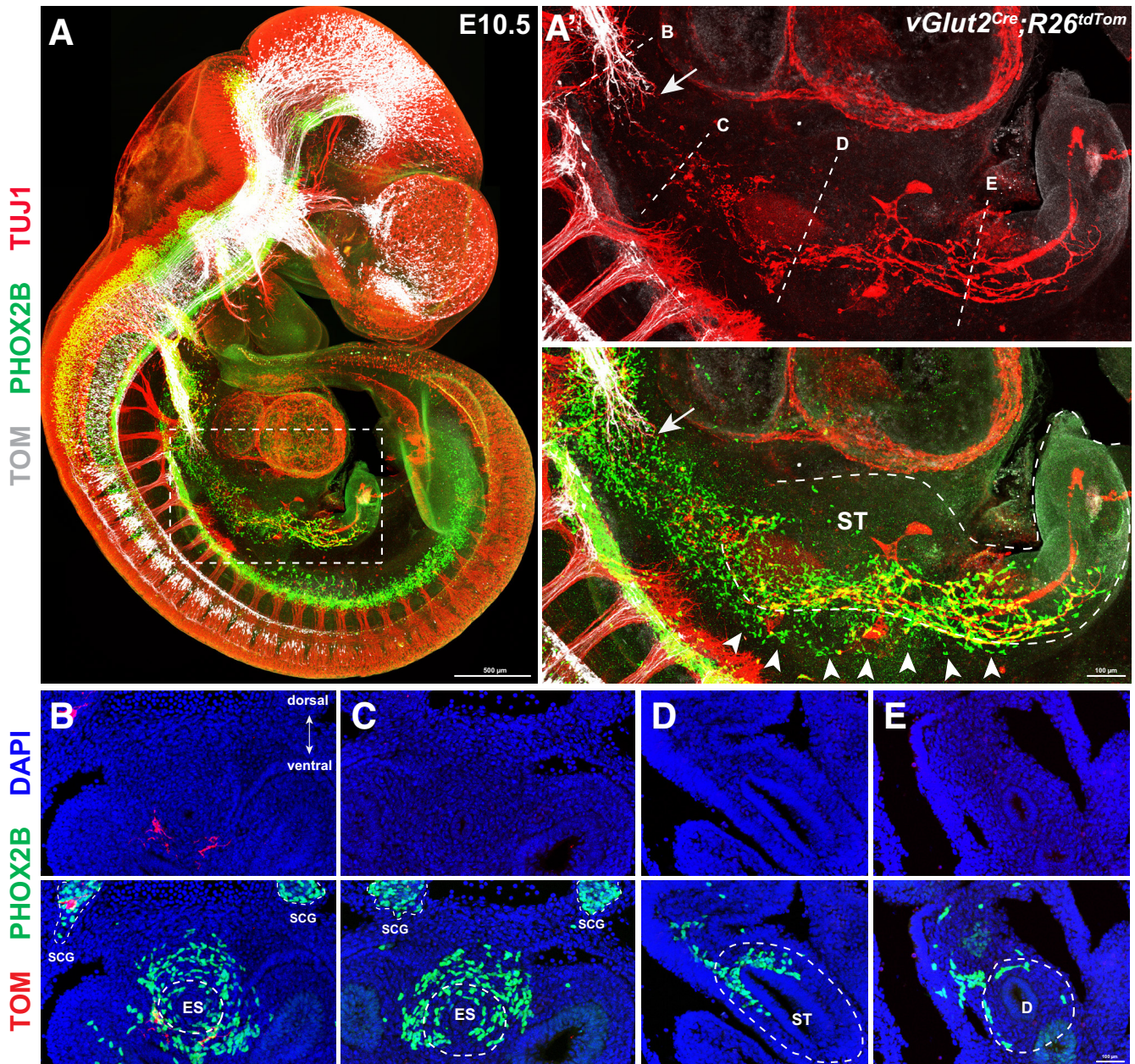
Figure 4. A subset of vNCCs migrate along the mesentery at E10.5. (*A*) Representative image of E10.5 *vGlut2^Cre^;R26^tdTom^* embryos with PHOX2B and TUJ1 staining. (*A'*) Magnified view of the *boxed area* in panel *A*. *Arrows* indicate pioneer vagus axons (TOM$^+$/TUJ1$^+$). *Dotted lines* mark the sites of the sections shown in panels *B–E*, and the presumptive margins of the gut, respectively. Note the presence of mNCCs (*arrowheads*) within the mesentery. (*B–E*) Transverse sections showing the distribution of vNCCs within the dorsal mesentery of the (*B* and *C*) esophagus, (*D*) stomach, and (*E*) duodenum. Note the presence of fewer PHOX2B$^+$ cells in the antimesenteric side of the gut. *Dotted lines* indicate the presumptive margins of the gut. D, duodenum; DAPI, 4′,6-diamidino-2-phenylindole; ES, esophagus; SCG, sympathetic chain ganglion; ST, stomach.

ask whether mNCCs are the embryonic origin of the segmental ENS in SSHD. Given that SSHD is a rare and controversial clinical condition, we first searched for SSHD cases by preparing biopsy specimens from HSCR patients using the previously described Swiss-roll technique (Figure 8*A*),[55] followed by H&E staining to comprehensively identify enteric neurons within the aganglionic gut (Figure 8*B–F'*). Two SSHD cases were identified from 183 HSCR patients (1.09%; 2 of 183). We observed an innervated segment in the sigmoid colon of the first HSCR case with total colonic aganglionosis (TCA), and in the transverse colon of the second long-segment HSCR case (Table 1). To confirm the presence of neurons and glia within the aganglionic gut, we stained the Swiss-roll sections from the transitional zone and skip area of 1 SSHD patient with PHOX2B (a marker of enteric
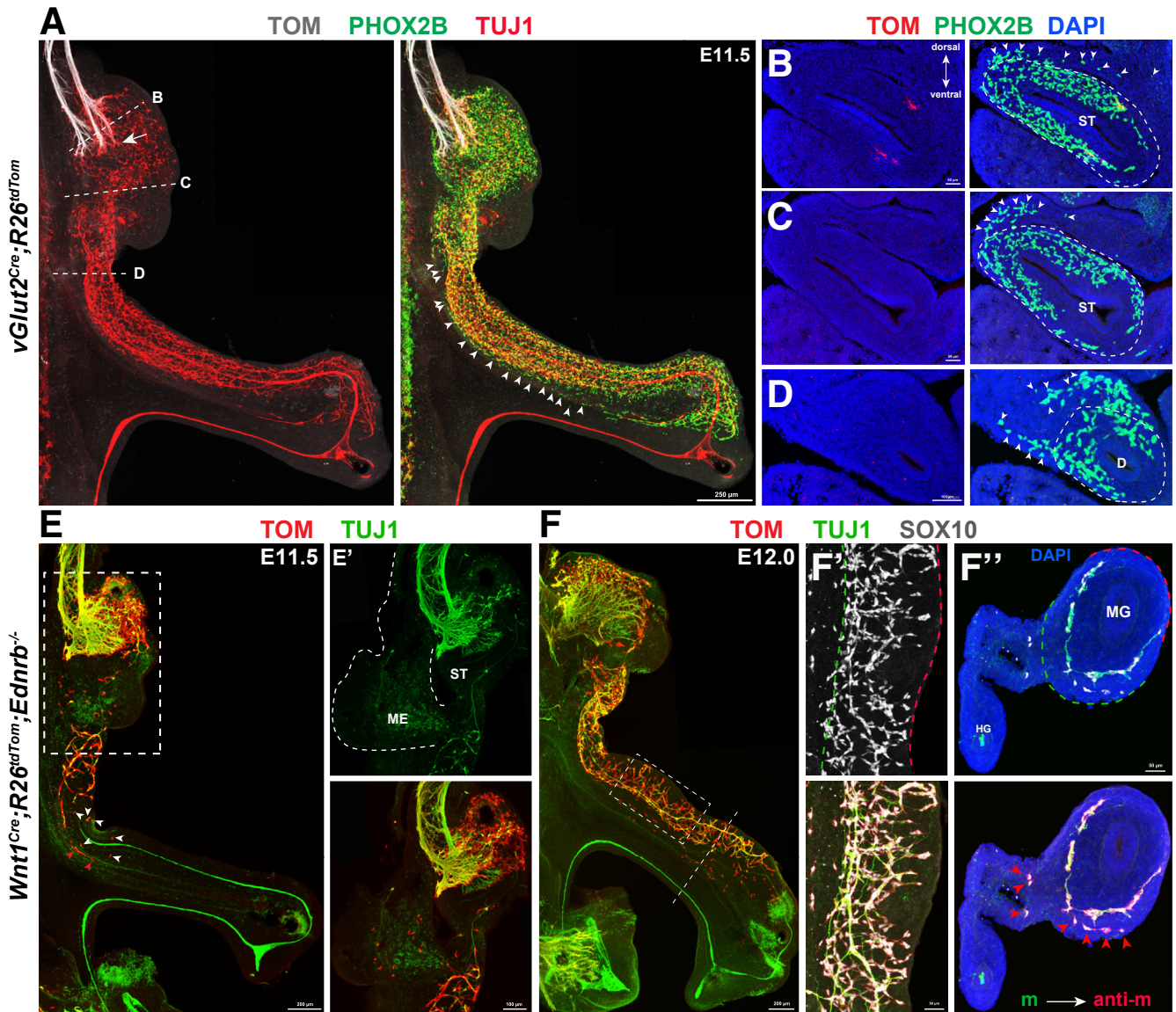
Figure 5. mNCCs and tmNCCs might be the same population of descending vNCCs. (*A*) Representative image of E11.5 *vGlut2^Cre^;R26^tdTom^* guts with PHOX2B and TUJ1 staining. *Dotted lines* mark the sites of sections shown in panels *B–D*, and *arrowheads* indicate mNCCs within the mesentery. Vagus axons project into the stomach at E11.5 (*arrow*). (*B–D*) Transverse sections showing the presence of PHOX2B⁺ mNCC (*arrowheads*) in the mesentery. Note fewer cells in the antimesenteric side of the bowel. (*E*) Whole-mount preparation of an E11.5 gut from *Wnt1^Cre^;R26^tdTom^;Ednrb^-/-^* embryos showing scattered NCC clumps within the aganglionic gut (*arrowheads*). (*E'*) High magnification of the boxed area in *E*. The same sample as shown in panel *E*, showing the presence of mNCCs in the isolated mesentery. (*F*) Whole-mount preparation of the gut from E12.0 *Wnt1^Cre^;R26^tdTom^;Ednrb^-/-^* embryos. (*F'*) Magnified *boxed area* in panel *F* showing the mesenteric-to-antimesenteric distribution of eNCCs within the midgut. (*F''*) Transverse section at the level indicated by the *dotted line* in panel *F*. *Arrowheads* indicate TOM⁺/SOX10⁺ mNCCs. (*F'* and *F''*) *Green dotted lines* and *red dotted lines* mark the mesenteric and antimesenteric borders, respectively. anti-m, antimesenteric border; D, duodenum; DAPI, 4′,6-diamidino-2-phenylindole; HG, hindgut; m, mesenteric border; ME, mesentery; MG, midgut; ST, stomach.

neurons) and S100 (a marker of enteric glia). In contrast to the transitional zone, where ganglia were distributed in a rostrocaudal gradient along the gut (Figure 8*G–J*), several myenteric ganglia, containing both neurons and glia, were detected within the aganglionic colon (Figure 8*K–L''*). Meanwhile, no PHOX2B⁺ neurons were present within the hypertrophic nerve trunks along the myenteric plexus (Figure 8*M*). Because the Swiss-roll

technique provided a relatively limited view of the complete aganglionic intestine, it was possible that the identified small clusters of ganglia within the aganglionic intestine might be connected to the most advanced enteric neurons, and these connecting neurons were not present in the selected Swiss-roll sections.[56] However, the skip segments within the aganglionic intestine of the 2 SSHD cases were both located far distal to the most

advanced enteric neurons, making it much less likely that the sparse connecting neurons might be missed via Swiss-roll technique. Thus, SSHD is a definite rare clinical entity.

We then proceeded to test whether SSHD-like phenotypes could be recapitulated in postnatal $Wnt1^{Cre};R26^{tdTom};Ednrb^{-/-}$ mice. We first monitored the spatiotemporal formation of the segmental ENS within the
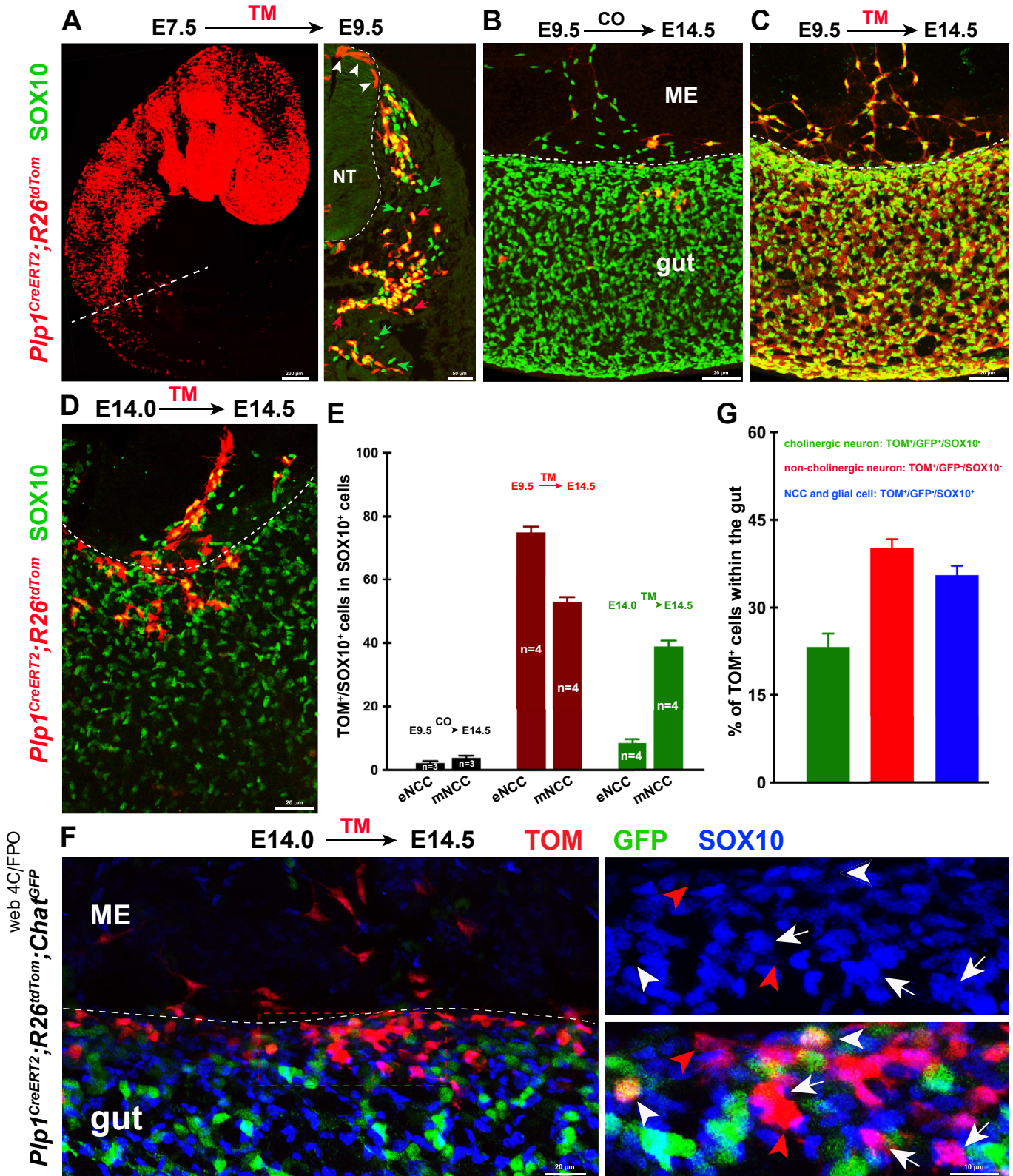
aganglionic $Ednrb^{-/-}$ guts from E14.5 to postnatal day 30 (P30). Although a few scattered NCC clumps were distributed along the aganglionic gut at E14.5, the mNCC-occupied areas increased with development, leading to the occurrence of ganglionic segments within the aganglionic gut of postnatal $Wnt1^{Cre};R26^{tdTom};Ednrb^{-/-}$ mice (Figure 9). To examine the cellular components within the segmental ENS, whole-mount staining of the distal gut from P0 $Wnt1^{Cre};R26^{tdTom};Ednrb^{-/-}$ mice was performed to detect TUJ1, SOX10, and PHOX2B (Figure 10A and A'). These markers were used to distinguish enteric neurons (TUJ1$^+$/PHOX2B$^+$/SOX10$^-$), enteric glia (TUJ1$^-$/PHOX2B$^-$/SOX10$^+$), NCCs (TUJ1$^-$/PHOX2B$^+$/SOX10$^+$), extrinsic axons (TUJ1$^+$), and axon-associated SCPs (TUJ1$^-$/PHOX2B$^-$/SOX10$^+$). NCCs, enteric neurons, and enteric glia were detected simultaneously within the segmental ENS (Figure 10B). Meanwhile, SCPs invariably were associated intimately with extrinsic axons within the aganglionic gut, and no NCC clumps were detected in the vicinity around the extrinsic axons (Figure 10A and A').

Consistent with previous analyses that most human SSHD cases are cases of TCA (Table 1), 90.32% (28 of 31) of the mice with innervated skip areas showed TCA, and the remaining mice presented with long-segment intestinal aganglionosis (Figure 10C). Surprisingly, in contrast to the lower incidence of SSHD in HSCR patients, innervated skip areas were detected within the majority of the aganglionic intestines of $Wnt1^{Cre};R26^{tdTom};Ednrb^{-/-}$ mice (55.36%; 31 of 56) (Figure 10C). Meanwhile, different from the restriction of aganglionosis to the distal colon of $Ednrb$-deficient mice,[50,57] the majority of $Wnt1^{Cre};R26^{tdTom};Ednrb^{-/-}$ mice (80.36%; 45 of 56) showed aganglionosis extending all the way through the colon and into the distal small bowel (Figure 10C). Because Wnt1 signaling has been implicated to play roles in neural crest lineage generation,[58,59] together with the finding that Wnt1–Cre transgenic mice show phenotypes in multiple aspects of midbrain development,[60] one potential explanation for the discrepant extent of aganglionosis between $Wnt1^{Cre};R26^{tdTom};Ednrb^{-/-}$ and $Ednrb^{-/-}$ mice might be that $Wnt1$ and $Ednrb$ act synergically to control the development of the ENS. To gain evidence of this speculation, we examined the extent of aganglionosis of $Ednrb^{-/-}$ mice with the same genetic background as that of $Wnt1^{Cre};R26^{tdTom};Ednrb^{-/-}$ mice. In line with previous observations,[50] a much lesser extent of aganglionosis was

observed in $Ednrb^{-/-}$ mice compared with that of $Wnt1^{Cre};R26^{tdTom};Ednrb^{-/-}$ mice (Figure 10C). Thus, additional $Wnt1$ mutation in $Ednrb^{-/-}$ mice has significantly exacerbated the aganglionic phenotype, consequently highlighting the presence of skip segment within the aganglionic intestine.

Together, these findings strongly suggest that the segmental ENS in SSHD is derived from mNCCs.

Endothelin 3/Endothelin Receptor Type B , But Not Glial Cell-derived Neurotrophic Factor/RET, Signaling Pathway Might Play Roles in the Etiology of SSHD

RET signaling is critical for ENS development, and the inactivation of this pathway is the main cause of HSCR.[61] We further established the $Wnt1^{Cre};R26^{tdTom};Ret^{-/-}$ line to examine the incidence of SSHD-like phenotypes in $Ret^{-/-}$ embryos. In line with previous observations,[62,63] all $Wnt1^{Cre};R26^{tdTom};Ret^{-/-}$ embryos from E12.5 to E18.5 showed total intestinal aganglionosis, except for an occasional TCA case (Figure 11A–C). In contrast to the high incidence of SSHD in $Wnt1^{Cre};R26^{tdTom};Ednrb^{-/-}$ mice, no enteric neurons were detected within the aganglionic $Ret^{-/-}$ intestines (Figure 11C), thus implicating that RET signaling might not be involved in the etiology of SSHD. Because Ret and endothelin receptor type B (EDNRB) both are expressed specifically in mNCCs, we speculated that glial cell-derived neurotrophic factor (GDNF) and endothelin 3 (EDN3), the ligands for Ret and EDNRB, respectively, might have distinctive expression patterns within the GI tract. To test this speculation, we performed double fluorescence in situ hybridization, in combination with SOX10 detection, to examine the expression levels of $Gdnf$ and $Edn3$ in the gut at E14.5, the stage at which mNCCs undergo mesentery–gut migration. In addition to diffuse weak signals within the mesentery, $Gdnf$ and $Edn3$ indeed showed different expression patterns throughout the whole gut. $Edn3$ consistently was localized mainly in the serosal epithelium and the outermost layers of the splanchnopleural mesenchyme, while $Gdnf$ was highly expressed in the developing muscle layers around the NCCs (Figure 11D and D'). The distinctive expression patterns of $Gdnf$ and $Edn3$ thus suggested that EDN3 most likely participates in the regulation of mNCC

Figure 6. (See previous page). **mNCCs migrate into the gut to contribute to the ENS.** (A) Temporal tracing of NCCs in $Plp1^{CreERT2};R26^{tdTom}$ embryos from E7.5 to E9.5. The dotted line marks the site of section on the right. Arrowheads indicate TOM$^+$/SOX10$^-$ premigratory NCCs within the neural tube (NT). Green arrows and red arrows indicate TOM$^-$/SOX10$^+$ and TOM$^+$/SOX10$^+$ migratory NCCs, respectively. (B and C) Immunofluorescent detection of SOX10 and TOM in the midguts of E14.5 $Plp1^{CreERT2};R26^{tdTom}$ embryos after corn oil (CO) and TM injection at E9.5. Corn oil–induced control midgut showed much lower basal CreERT leakage, thus CreERT leakage does not hamper lineage tracing of NCCs. (D) Representative midgut from E14.5 $Plp1^{CreERT2};R26^{tdTom}$ embryos with SOX10 staining. Temporally traced mNCCs seem to be undergoing mesentery–gut migration. (E) Quantification of the proportion of TOM$^+$/SOX10$^+$ cells relative to the total number of SOX10$^+$ cells. Note the higher tracing efficiency of mNCCs in embryos with 12-hour tracing from E14.0 (n indicates the number of samples). (F) Representative midgut segment from E14.5 $Plp1^{CreERT2};R26^{tdTom};Chat^{GFP}$ embryos with 12 hours of tracing. Traced mNCCs invade the gut and differentiate into cholinergic (TOM$^+$/GFP$^+$/SOX10$^-$; white arrowheads) and noncholinergic (TOM$^+$/GFP$^-$/SOX10$^-$; red arrowheads) neurons. Arrows indicate NCCs or NCC-derived glia (TOM$^+$/GFP$^-$/SOX10$^+$). (G) Quantification of the percentage of traced mNCCs within the gut (n = 875 NCCs within the midgut from 5 embryos). ME, mesentery; NT, neural tube.

mesentery–gut migration, while GDNF/RET signaling is needed not only for the migration of eNCCs along the gut, but also for mNCCs to enter the gut.

To further determine the effect of the EDN3/EDNRB signaling pathway on mNCC development, we compared the numbers of mNCCs in $Wnt1^{Cre};R26^{tdTom}$ and
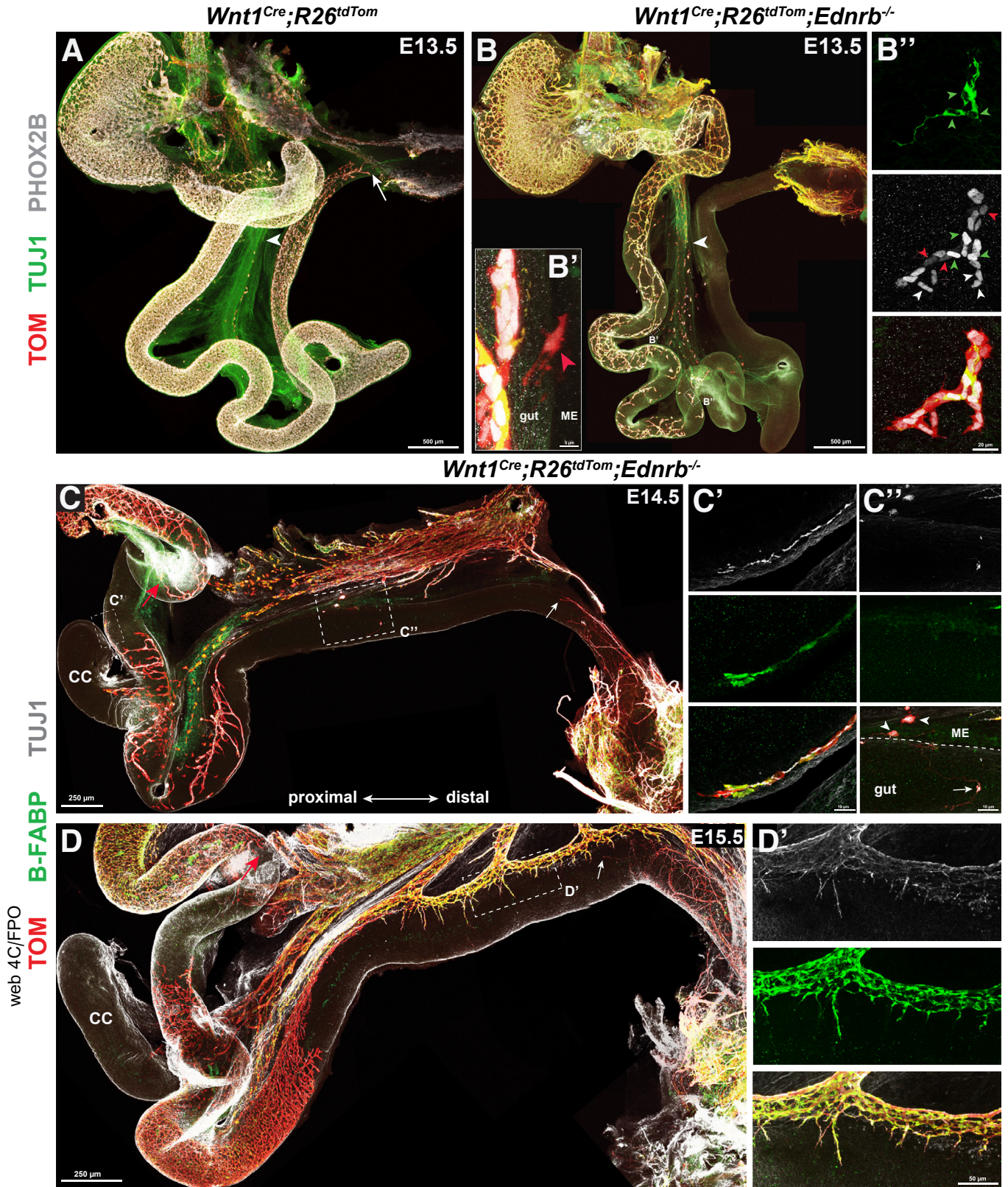
$Wnt1^{Cre}$;$R26^{tdTom}$;$Ednrb^{-/-}$ embryos between E12.5 and E14.5. Despite the substantial reduction in the total number of NCCs in $Wnt1^{Cre}$;$R26^{tdTom}$;$Ednrb^{-/-}$ embryos, we noticed that the decreased number of eNCCs was invariably accompanied by a concomitant significant increase in the number of mNCCs (Figure 11E–G). To determine whether mNCCs underwent premature neurogenesis in $Wnt1^{Cre}$;$R26^{tdTom}$;$Ednrb^{-/-}$ embryos, the whole GI tracts were stained for TUJ1 and TOM to trace mNCC-derived mesenteric neurons. Although a comparable number of TUJ1$^+$/TOM$^+$ neurons were detected within the $Ednrb^{-/-}$ gut mesentery (Figure 11H), the percentage of mNCC-derived neurons was significantly lower than that of $Wnt1^{Cre}$;$R26^{tdTom}$ embryos (Figure 11I). Thus, different from previous findings that EDN3 maintains the multipotency of NCCs by inhibiting their differentiation into neurons,[63,64] EDN3 signaling seemed to stimulate mNCCs to differentiate into mesenteric neurons.

In summary, the EDN3/EDNRB signaling pathway modulated the migration and differentiation of mNCCs, and might be involved in the etiology of SSHD.

Discussion

The present study showed that a subset of vNCCs migrate via the gut mesentery to make complementary contributions to the ENS. Integrating our findings with previous observations, we propose a modified model of ENS development as follows (Figure 12A and B). First, vNCCs migrate into the dorsal mesentery of the foregut (the esophagus, stomach, and duodenum). Second, the majority of vNCCs (ie, eNCCs) enter the foregut to migrate along the gut, with the remaining vNCCs (ie, mNCCs) proceeding to migrate along the gut mesentery. Third, during mesenteric migration, mNCCs continuously invade the gut to maintain the critical number of eNCCs for ENS formation. Because of the relatively slow migration of mNCCs and the considerably faster growth of the gut mesentery, the regions in which mNCCs invade the gut already are occupied by eNCCs. For this reason, mNCCs are indistinguishable from eNCCs. Based on this model, together with the recapitulated SSHD-like phenotypes in $Wnt1^{Cre}$;$R26^{tdTom}$;$Ednrb^{-/-}$ mice, we propose that mNCCs are the embryonic origin of the segmental ENS in SSHD. The gut mesentery in SSHD patients provides a favorable pathway for vNCCs, leading to an increased number of mNCCs undergoing mesentery–gut migration to

form a segmental ENS within the aganglionic bowel (Figure 12D).

Several hypotheses have been proposed surrounding the pathogenesis of SSHD. Later, we discuss our hypothesis in light of these proposed models. If the migration of eNCCs along the gut is accompanied by interactions between eNCCs and gut mesenchymal cells, the most straightforward explanation for the segmental ENS is that the defective differentiation of eNCCs induces a discontinuous distribution of enteric neurons. This defective differentiation hypothesis is based mainly on the spatiotemporal expression patterns of some gut mesenchymal molecules, as exemplified by GDNF, which is expressed in the stomach and cecum in advance of the wavefront of Ret-expressing eNCCs.[65,66] In addition, high levels of EDN3 similarly are expressed in a restricted manner by mesenchymal cells of the cecum before and after the arrival of eNCCs.[67] In line with the expression pattern of EDN3, another study, by temporal manipulating expression of $Ednrb$ at different stages of embryogenesis, argued that EDN3 is temporally required for cecum colonization between E10.0 and E12.5.[68] Notwithstanding these studies, the spatiotemporal expression patterns of GDNF and EDN3 are not correlated with the locations of the segmental ENS. Given that SSHD-like phenotypes rarely are observed within the aganglionic intestines of $Gdnf$- and $Edn3$-deficient mice, together with the existence of long segmental aganglionic regions in most SSHD cases, defective differentiation of eNCCs in HSCR is less likely to result in segmental ENS.

The second potential origin of the segmental ENS has been hypothesized to be sNCCs. Under this hypothesis, the aganglionic zones are explained as a failure of vNCCs and sNCCs to merge together. However, sNCCs are unlikely to be the embryologic basis of SSHD for several reasons. First, sNCCs invade the hindgut either along the axons of neurons in the nerve of Remak (in chicken embryos) or along pelvic ganglion-arising axons (in mouse embryos).[31,32] Despite the phenotypic similarities between NCCs and SCPs, SCPs are distinguished by their intimate associations with neuronal axons, therefore raising the possibility that these axon-associated sNCCs are sacral SCPs. Consistent with this speculation, we detected axon-associated SCPs, but not independent NCCs or NCC-derived neurons, within the most distal aganglionic hindguts of $Ednrb^{-/-}$ and $Ret^{-/-}$ mice. Thus, the axon-associated sNCCs identified in mice and chickens are most likely SCPs. Second, although the

Figure 7. (See previous page). mNCCs migrate into aganglionic guts to contribute to the ENS. (A) Whole-mount preparation of an E13.5 $Wnt1^{Cre}$;$R26^{tdTom}$ gut. *Arrowhead* and *arrow* indicate pioneer extrinsic axons and the wavefront of eNCCs, respectively. (B) Whole-mount preparation of an E13.5 $Wnt1^{Cre}$;$R26^{tdTom}$;$Ednrb^{-/-}$ gut showing the loss of typical rostral–caudal eNCC chain integrity along the gut. The *arrowhead* indicates pioneer extrinsic axons. (B') Magnification of the *boxed area* in panel B, showing 1 mNCC (*arrowhead*) migrating in or out of the midgut. (B'') Magnified view of another *boxed area* in panel B, showing a solitary NCC clump within the midgut. NCC-derived neurons (TOM$^+$/PHOX2B^{strong}/TUJ1$^+$), NCC-derived glia (TOM$^+$/PHOX2B^{weak}/TUJ1$^-$), and NCCs (TOM$^+$/PHOX2B^{strong}/TUJ1$^-$) are indicated by *green arrowheads*, *red arrowheads*, and *white arrowheads*, respectively. (C and D) Segmental ENS within the aganglionic guts of E14.5 and E15.5 $Wnt1^{Cre}$;$R26^{tdTom}$;$Ednrb^{-/-}$ embryos. *Red arrows* indicate the migratory wavefront of eNCCs. *White arrows* indicate pioneer pelvic ganglion-arising axons within the hindgut. (C') Magnified view of the *boxed area* in panel C, showing mNCC-derived neurons (TOM$^+$/TUJ1$^+$) and glia (TOM$^+$/B-FABP$^+$). (C'') Magnified view of another *boxed area* in panel C showing mesenteric (*arrowheads*) and enteric (*arrow*) neuronal clumps. (D') Magnified view of the *boxed area* in panel D, showing extrinsic axon-associated SCPs (TOM$^+$/B-BFAP$^+$). CC, cecum; ME, mesentery.
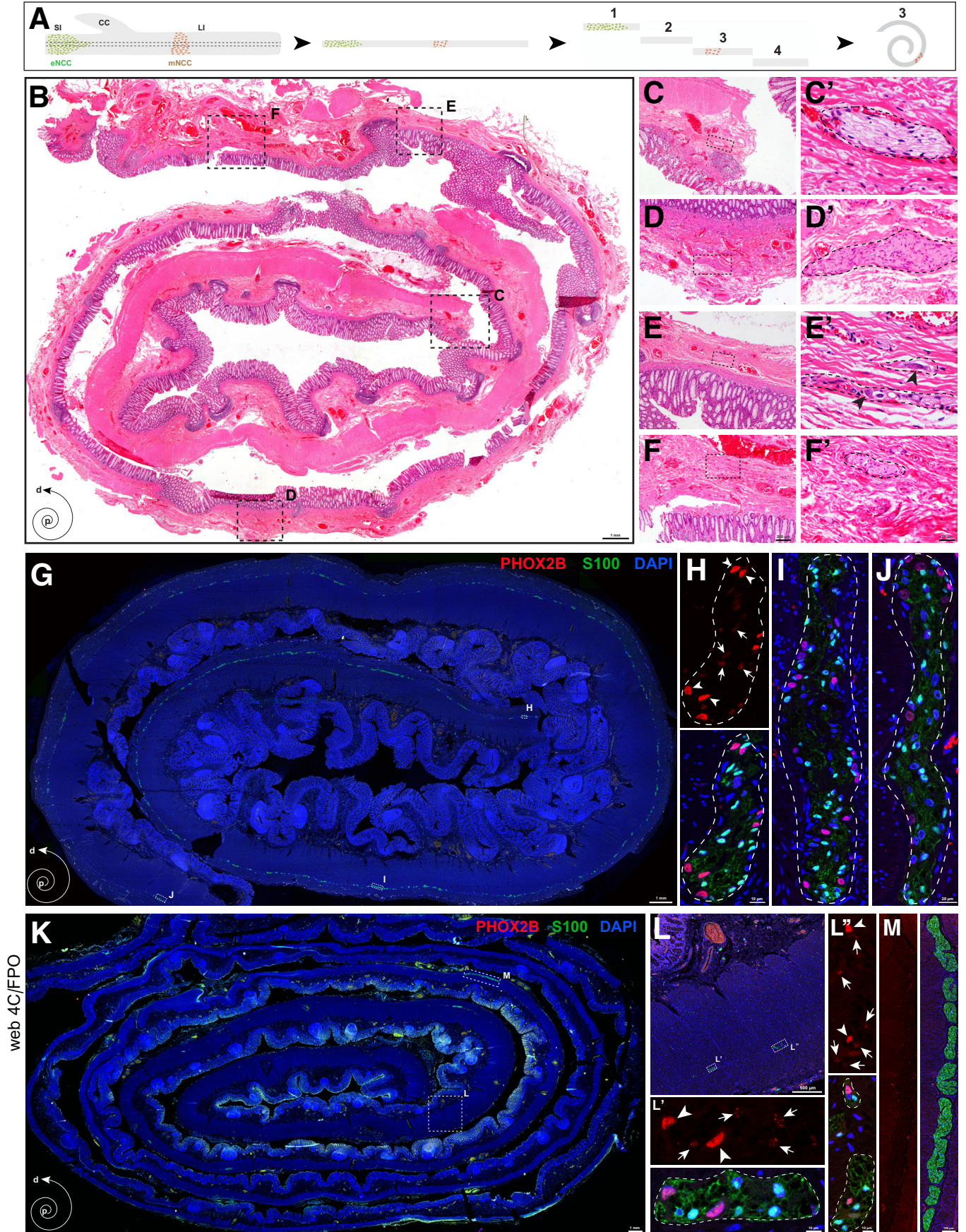
sNCC model might provide an explanation for the skip areas in the rectum, this model could not provide a convincing explanation for the location of the most common skip areas within the ileocecal region (Table 1). Third, given the contribution of sNCCs to the ENS, skip areas with enteric neurons are expected to be detected within the distal intestine of most HSCR patients. By contrast, although previous studies have shown that the numbers of sNCC-derived neurons are increased slightly in the aganglionic hindgut of chicken embryos,[31,69] aganglionosis invariably were detected within the distal intestines of genetic mutant mice and HSCR patients, thus arguing against this sNCC theory. Nevertheless, a possible explanation for the failure of sNCCs to compensate for the loss of enteric neurons in HSCR patients might be that the genetic environmental factors that cause aganglionosis similarly affect the development of sNCCs, and this speculation remains to be addressed.

During migration through the cecum, a stream of pioneer eNCCs migrates extramurally along the mesenteric border of the cecum, invades into the proximal colon, and backfills the cecum.[33,34] Based on this unique behavioral pattern of eNCCs through the cecum, together with the defective extramural migration of NCCs in *Edn3* mutant embryos, Kapur et al[17] proposed that the segmental ENS might arise from these backfilling eNCCs. Under this hypothesis, skip segments jointly result from the defective backfilling of eNCCs and the delayed migration of eNCCs along the proximal intestine. Consistent with this model, our data provided compelling evidence that vNCCs migrate directly into the mesentery, implying that extramural migrating NCCs are most likely the same population of mNCCs. Moreover, the preferential migration of *Ednrb*^{-/-} vNCCs along the gut mesentery is consistent with the defective migration of NCCs along the mesenteric border of the cecum of *Edn3*^{-/-} embryos. Thus, this backfill model could be incorporated into our mNCC model to better explain the pathogenesis of SSHD.
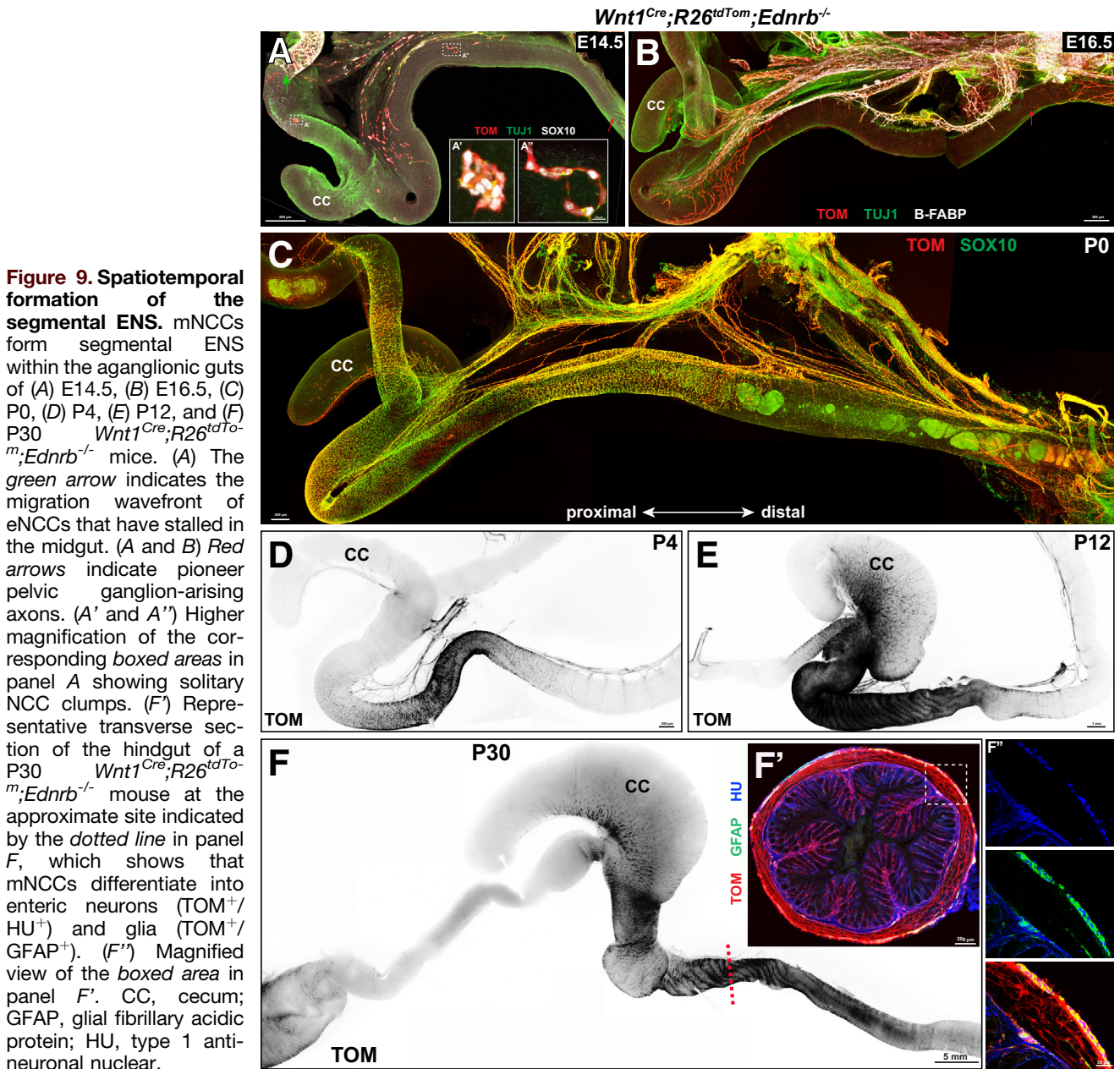
A recent time-lapse tracing study showed that a population of midgut eNCCs migrated across the mesentery to the hindgut, serving as the principal source of the colonic ENS. Takahashi et al[36] speculated that the aganglionic gaps in SSHD patients might indicate a failure of the eNCCs and tmNCCs to merge. Similar to the backfill model, although the tmNCCs could account for skip areas in the postcecum gut, it is unlikely that tmNCCs are the

origin of the segmental ENS within the ileum, cecum, and rectum (Table 1). Moreover, based on the developmental anatomy of human intestine, recent work has implicated that transmesenteric migration is unlikely to occur in normal human embryogenesis.[70] The main difference between our model and the tmNCC model lies in the hypothesized origin of the NCCs within the gut mesentery. Based on the location of mNCCs within the gut mesentery, Nishiyama et al[35] preliminarily concluded that tmNCCs were derived from midgut eNCCs. In contrast, our results showed that removal of the eNCCs from the midgut of *Ednrb*^{-/-} embryos did not induce a concomitant loss of NCCs within the mesentery, thus excluding the possibility that tmNCCs arise from midgut eNCCs in *Ednrb*^{-/-} embryos. Therefore, our model not only provided convincing evidence for the origin of the mNCCs, but also explained the variable positions of the skip areas better than the tmNCC model.

Zonal aganglionosis is another rare variant of HSCR and is characterized by a segment of aganglionic bowel that is preceded and followed by bowel with normal innervation.[15,71] Multiple skip areas have been detected within the aganglionic intestine of some SSHD patients (Table 1). Consequently, SSHD is sometimes referred to as "double zonal aganglionosis."[5] Although typical zonal aganglionosis–like phenotypes were not detected in our study, scattered mNCC-derived NCC clumps occasionally occurred within the aganglionic gut of *Wnt1*[Cre];*R26*[tdTom];*Ednrb*^{-/-} embryos during early embryonic stages. Because the phenotypic discrepancies between zonal aganglionosis and SSHD include the locations, lengths, and numbers of skip areas within the aganglionic intestine, and because these differences could be explained by the variable contribution of mNCCs to the segmental ENS, it is likely that mNCCs are the embryonic origin of the distal ganglionic segment of zonal aganglionosis.

The EDN3/EDNRB and GDNF/RET signaling pathways have been shown to regulate eNCC migration both independently and cooperatively. Higher expression levels of GDNF and EDN3 are detected in the cecum and colon after E14.5 when the gut has been fully colonized,[67,72] implicating that GDNF and EDN3 play additional roles in ENS development after the gut has been completely colonized by eNCCs. Although the *Ret* mutation is the most common genetic cause of HSCR, our data showed that the incidence of SSHD in *Ret*^{-/-} mice was much lower than that in

Figure 8. (*See previous page*). **Presence of enteric neurons within the human aganglionic intestines.** (*A*) Schematic illustration for preparation of human intestines with the Swiss-roll technique. (*B*) Representative Swiss-roll colonic section with H&E staining. (*C–F*) Magnified views of the corresponding *boxed areas* in panel *B*. (*C'–F'*) Magnified views of the corresponding *boxed areas* from panels *C–F*. The *dotted lines* mark the boundaries of hypertrophic nerve trunks. (*E'*) *Arrowheads* indicate enteric neurons within the ganglia. (*G*) Representative Swiss-roll section from the transition zone of an SSHD patient. (*H–J*) Magnified views of the corresponding areas in panel *G*, showing the presence of both PHOX2B+ neurons and S100+ glia within the ganglia. (*H*) *Arrows* and *arrowheads* indicate glia and neurons, respectively. Note the weak PHOX2B signals in S100+ glia. *Dotted lines* indicate the boundaries of individual enteric ganglia. (*K*) Representative Swiss-roll colonic section from the skip area of the same SSHD patient as in panel *G*. (*L–L''*) Magnified views of the corresponding areas showing the presence of PHOX2B+ neurons (*arrowheads*) and S100+ glia (*arrows*) within the aganglionic colon. Note the weak PHOX2B signals in S100+ glia. (*M*) Magnified view of the *boxed area* in panel *K* showing hypertrophic nerve trunks. No PHOX2B+ neurons are present within these ganglia. CC, cecum; d, distal; DAPI, 4′,6-diamidino-2-phenylindole; LI, large intestine; p, proximal; SI, small intestine.

Figure 9. Spatiotemporal formation of the segmental ENS. mNCCs form segmental ENS within the aganglionic guts of (*A*) E14.5, (*B*) E16.5, (*C*) P0, (*D*) P4, (*E*) P12, and (*F*) P30 $Wnt1^{Cre};R26^{tdTom};Ednrb^{-/-}$ mice. (*A*) The *green arrow* indicates the migration wavefront of eNCCs that have stalled in the midgut. (*A* and *B*) *Red arrows* indicate pioneer pelvic ganglion-arising axons. (*A'* and *A''*) Higher magnification of the corresponding *boxed areas* in panel *A* showing solitary NCC clumps. (*F'*) Representative transverse section of the hindgut of a P30 $Wnt1^{Cre};R26^{tdTom};Ednrb^{-/-}$ mouse at the approximate site indicated by the *dotted line* in panel *F*, which shows that mNCCs differentiate into enteric neurons (TOM⁺/HU⁺) and glia (TOM⁺/GFAP⁺). (*F''*) Magnified view of the *boxed area* in panel *F'*. CC, cecum; GFAP, glial fibrillary acidic protein; HU, type 1 anti-neuronal nuclear.

$Ednrb^{-/-}$ mice. Although the lower incidence of SSHD in $Ret^{-/-}$ mice could be owing to the profound effect of *Ret* deficiency on the development of the ENS, the distinctive expression patterns of *Gdnf* and *Edn3* along the GI tract implicate the EDN3/EDNRB, but not the GDNF/RET, signaling pathway might be involved in the pathogenesis of SSHD. This speculation was in agreement with the recent identification of an *Ednrb* mutation in SSHD patients.[27] In contrast to *Ret* coding mutations, which account for 7%–35% of sporadic HSCR cases and 50% of familial HSCR cases,[73] mutations in the *Ednrb* gene are found in 7% of all HSCR patients,[74] potentially providing insights into the underlying reasons for the lower incidence of SSHD in HSCR patients. Although identifying the molecular pathways underlying the pathogenesis of SSHD is not the main focus of the present study, because SSHD-like phenotypes were recapitulated in the majority of $Ednrb^{-/-}$ mice, but not in $Ret^{-/-}$ mice, it would be of interest to investigate how the EDN3/EDNRB and GDNF/RET signaling pathways coordinately balance the relative abundances of eNCCs and mNCCs to ensure the proper development of the ENS in the future. Recently, Tang et al[75] performed whole-genome sequence analysis of patients with short-segment HSCR and identified additional HSCR relevant mutant genes, including *Erbb2* and *Bace2*. Thus, addressing the roles of *Erbb2* and *Bace2* in ENS development also would be one scientific direction to uncover the etiology of SSHD.
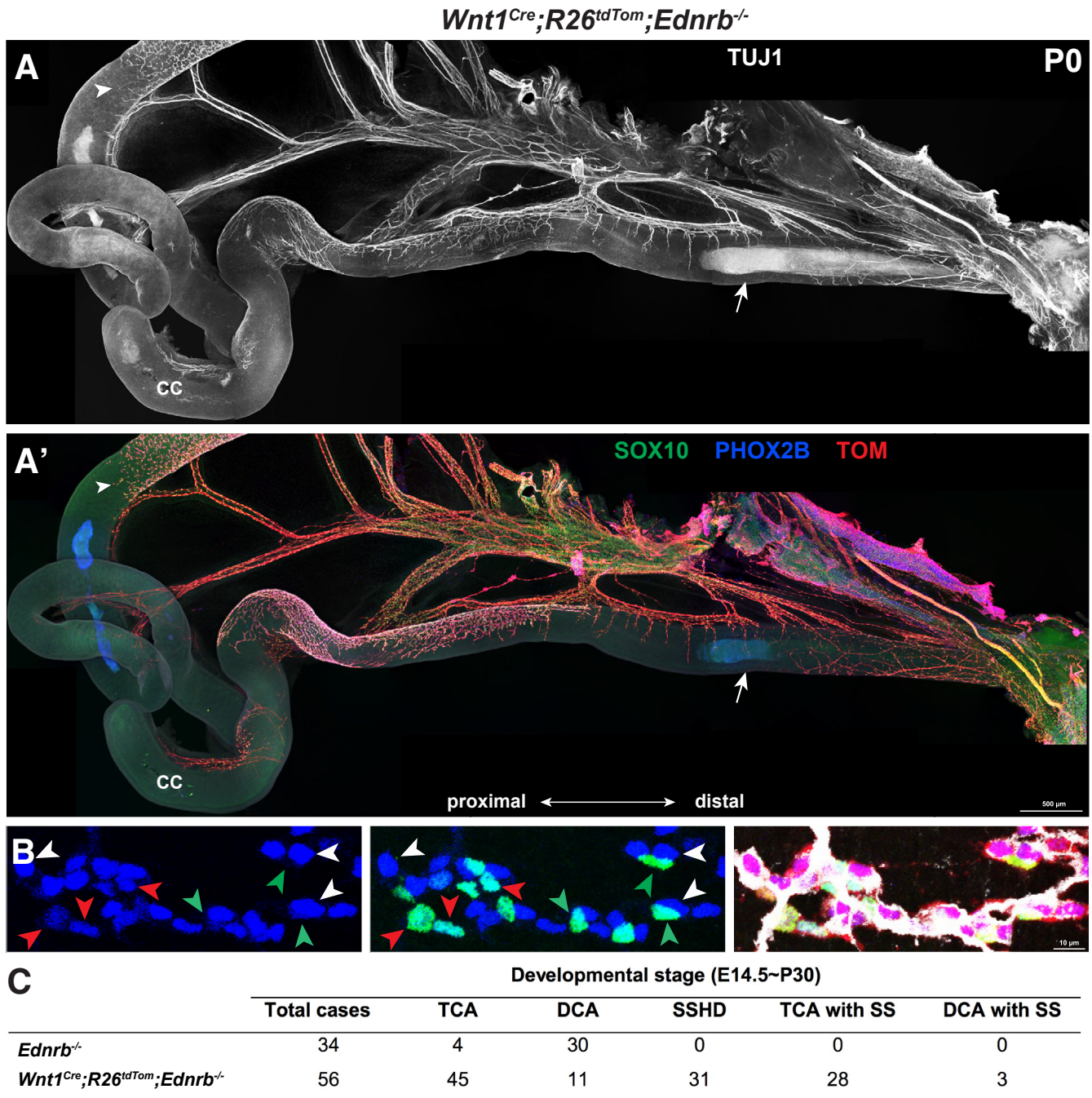
Figure 10. Presence of enteric neurons within the aganglionic gut of $Wnt1^{Cre};R26^{tdTom};Ednrb^{-/-}$ mice. (*A* and *A'*) Whole-mount views of the gut from a P0 $Wnt1^{Cre};R26^{tdTom};Ednrb^{-/-}$ mouse, showing an innervated segment within the aganglionic intestine. *Arrowheads* indicate the proximal wavefront of eNCCs and *arrows* indicate pioneer pelvic ganglion-arising axons within the distal hindgut. (*B*) Representative magnified view of the innervated segment, showing mNCC-derived neurons (TUJ1$^+$/PHOX2B$^+$/SOX10$^-$; *white arrowheads*), mNCC-derived glia (TUJ1$^-$/PHOX2B$^-$/SOX10$^+$; *green arrowheads*), and NCCs (TUJ1$^-$/PHOX2B$^+$/SOX10$^+$; *red arrowheads*). (*C*) Incidence of different types of aganglionosis within the guts of $Ednrb^{-/-}$ and $Wnt1^{Cre};R26^{tdTom};Ednrb^{-/-}$ mice. CC, cecum; DCA, distal colonic aganglionosis; DCA with SS, skip segment within DCA sample SS, skip segment; TCA, total colonic aganglionosis; TCA with SS, skip segment within TCA sample.

Materials and Methods
### Mouse Lines and Preparation of Mouse Samples

All mouse experimental procedures were approved by the Animal Care and Use Committee of Zhejiang University.

All the mouse lines used in our study were maintained on a C57BL/6 genetic background. The mice were maintained in a specific pathogen-free environment and fed with auto-clavable natural-ingredient diets (Xietong Shengwu, Lab

C

Developmental stage (E12.5 ~ E18.5)

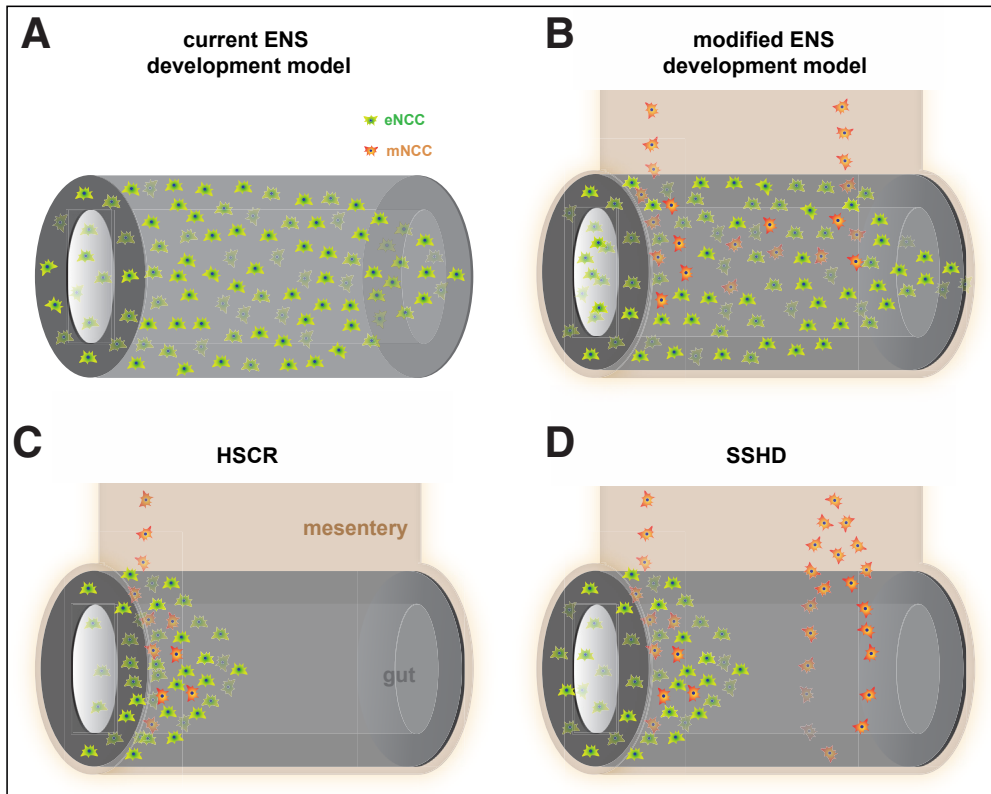|	Total cases	TA	TCA	DCA	SSHD	TCA with SS	DCA with SS
$Wnt1^{Cre};R26^{tdTom};Ret^{-/-}$	35	34	1	0	0	0	0
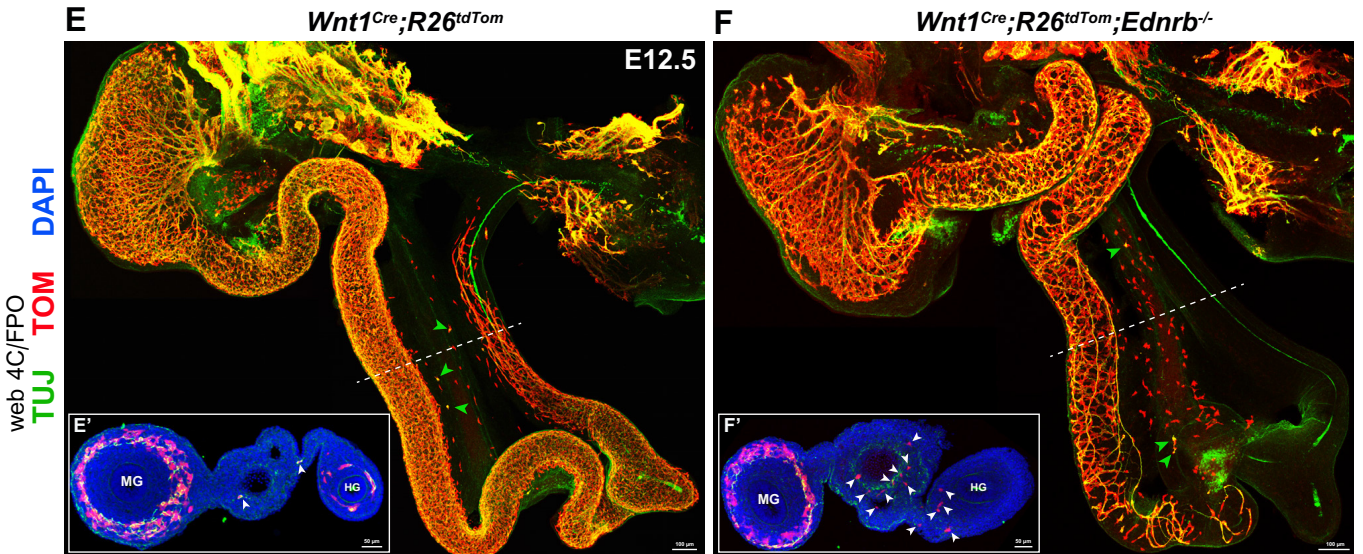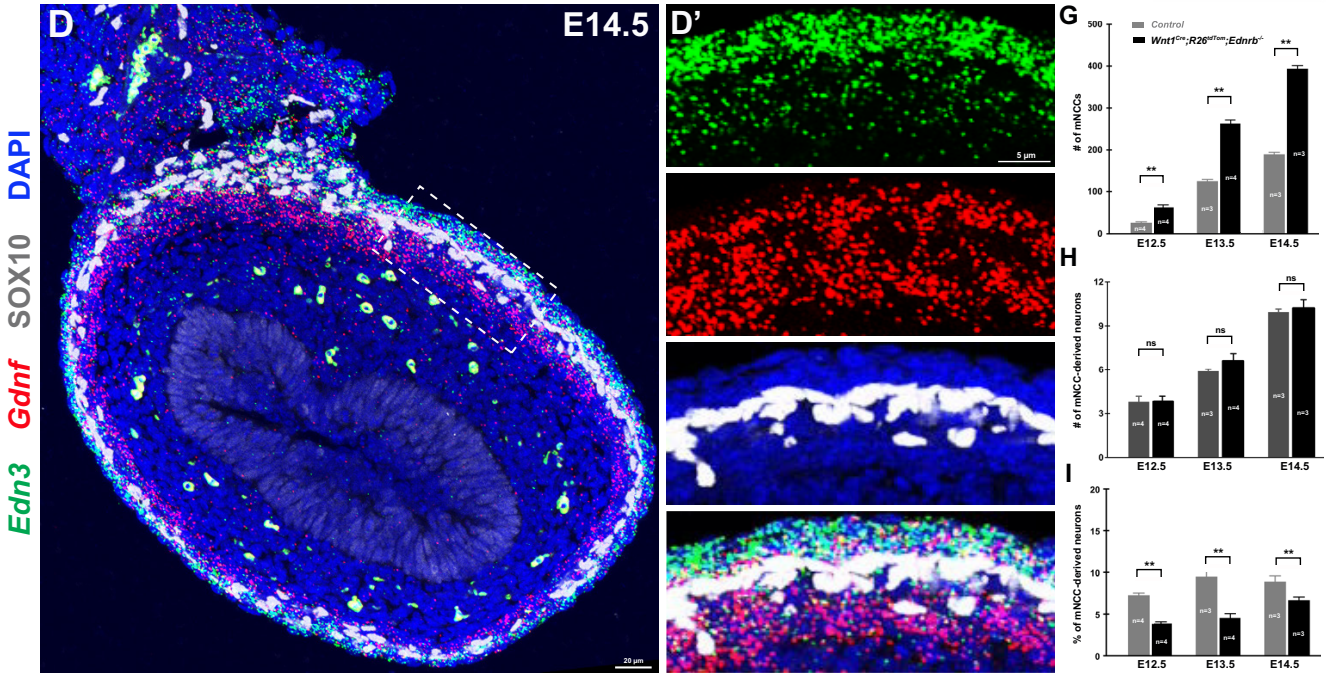
Figure 12. mNCCs are the embryonic origin of segmental ENS in SSHD. (*A*) Schematic model of current ENS development. vNCCs invade the foregut and migrate rostrocaudally to colonize the gut. (*B*) Model of modified ENS development. mNCCs migrate along the gut mesentery and undergo mesentery–gut migration to make a complementary contribution to the eNCC pool. (*C*) Pathogenic model of HSCR. Defective migration of both eNCCs and mNCCs jointly results in aganglionosis in the distal bowel. (*D*) Pathogenic model of SSHD. mNCCs preferentially migrate via the gut mesentery to form segmental ENS within the aganglionic gut.

mice diet 1010010). The following mouse lines were obtained from The Jackson Laboratory (Bar Harbor, ME): $Wnt1^{Cre}$ (JAX 022137), $Plp1^{CreERT2}$ (JAX 005975), $R26^{tdTom}$ (JAX 007909), $Phox2b^{FLP}$ (JAX 022407), $R26^{FLTG}$ (JAX 026932), $Chat^{Cre}$ (JAX 006410), $Chat^{GFP}$ (JAX 007902), Vip^{Cre} (JAX 010908), $vGlut2^{Cre}$ (JAX 016963), $vGat^{Cre}$ (JAX 016962), $Ednrb^{+/-}$ (JAX 003295), and $Ret^{+/-}$ (JAX 009085). The $Nestin^{GFP}$ line was obtained from the RIKEN BioResource Center (RBRC06355; TsukubaT, Japan). Dbh^{Cre} mice were generous gifts from Günther Schütz (German Cancer Research Center, Heidelberg, Germany).[77] Tamoxifen (T5648; Sigma-Aldrich, St. Louis, MO) was dissolved in corn oil (C8267; Sigma, St. Louis, MO) for lineage-tracing experiments. Pregnant females were injected intraperitoneally with a concentration ranging from 30 to 150 μg per gram of body weight for different efficiencies of genetic tracing. Whole embryos and the gastrointestinal tracts were fixed in 4% paraformaldehyde in phosphate-buffered saline (PBS) for 2–24 hours according to tissue sizes at room temperature. Then, the samples were either embedded in OCT media (45830; HistoLab, Askim, Sweden) for cryostat sectioning or kept in PBS for whole-mount staining.

Collection and Preparation of Human Samples

After approval by the Scientific Ethics Committee of The Wuhan Children's Hospital, intestinal biopsy specimens from HSCR patients undergoing bowel resections were collected and prepared with the Swiss-roll technique as

Figure 11. (*See previous page*). EDN3/EDNRB, but not GDNF/RET, signaling pathway plays roles in the migration and differentiation of mNCCs. (*A*) Representative image of an E12.5 $Wnt1^{Cre};R26^{tdTom};Ret^{-/-}$ gut showing aganglionosis along the whole gut. (*B*) Representative image of the distal hindgut from an E18.5 $Wnt1^{Cre};R26^{tdTom};Ret^{-/-}$ embryo. No ganglionic segment exists within the aganglionic gut. (*C*) Incidence of different types of aganglionosis within the gut of $Wnt1^{Cre};R26^{tdTom};Ret^{-/-}$ embryos. (*D*) Representative section of an E14.5 midgut with *Edn3* and *Gdnf* double-fluorescence in situ hybridization combined with SOX10 staining. (*D'*) Magnified view of the *boxed area* in panel *D*. (*E* and *F*) Whole-mount preparations from E12.5 $Wnt1^{Cre};R26^{tdTom}$ and $Wnt1^{Cre};R26^{tdTom};Ednrb^{-/-}$ embryos. Note the increased number of mNCCs within the $Ednrb^{-/-}$ gut mesentery. *Green arrowheads* indicate mNCC-derived neurons. (*E'* and *F'*) Transverse sections at the levels indicated by the *dotted lines*. *Arrowheads* indicate mNCCs. (*G*) Quantification of the number of mNCCs within the entire gut mesentery from *Control* and $Ednrb^{-/-}$ embryos (n indicates the number of samples). (*H*) Quantification of the number of mNCC-derived neurons within the entire gut mesentery from *Control* and $Ednrb^{-/-}$ embryos (n indicates the number of samples). (*I*) Quantification of the percentage of mNCC-derived neurons (n indicates the number of samples). (*G–I*) **$P < .01$; ns, not significant. CC, cecum; DAPI, 4′,6-diamidino-2-phenylindole; DCA, distal colonic aganglionosis; DCA with SS, skip segment within distal colonic aganglionosis sample; HG, hindgut; MG, midgut; SS, skip segment; TA, total aganglionosis; TCA, total colonic aganglionosis; TCA with SS, skip segment within total colonic aganglionosis sample.

previously described.[55] Briefly, the intestines were divided into several segments and each segment was cut open longitudinally along the mesenteric line. Then the segments were rolled up with a toothpick to form a Swiss roll. Finally, the intestine samples were fixed in 10% formalin prepared in PBS overnight at room temperature for paraffin embedding.

Staining Procedures

Whole-mount staining was performed as described previously.[77] Tissues were isolated and fixed in 4% paraformaldehyde/PBS for 6–24 hours according to tissue sizes at room temperature, followed by further fixation with Dent's solution (methanol:dimethyl sulfoxide 4:1) for 3–24 hours at room temperature. Primary antibodies and secondary antibodies were applied in 1% bovine serum albumin/PBS-Triton solution (0.5% Triton X-100; 9002-93-1; Sigma-Aldrich, St. Louis, MO) for 36–48 and 12–24 hours, respectively. After washing, the samples were cleared with BABB solution (benzyl alcohol:benzyl benzoate 1:2; Sigma) for imaging.

For immunofluorescence in frozen sections, embryos embedded in OCT were sectioned (30–60 μm) using a Leica Cryostat (LeicaCM1860; Leica biosystems, Nussloch, Germany). Primary and secondary antibody immunodetections were performed for 24 and 2 hours at room temperature, respectively, in 1% bovine serum albumin/PBS-Triton solution. Paraffin sections were cut at 5 μm and collected on charged slides to dry overnight at 65°C. After deparaffinization, paraffin sections underwent antigen retrieval in citrate buffer solution (10 mmol/L sodium citrate, 0.05% Tween-20, pH 6.0) at 100°C for 20 minutes. Then, the sections followed the same procedure as that for cryosection.

The following primary antibodies were used: rabbit anti-GFP (1:3000; A11122, ThermoFisher, Waltham, MA); chicken anti-GFP (1:3000; ab13970, Abcam, Cambridge, UK); rabbit anti-RFP (1:2000; ab62341, Abcam); goat anti-mCherry (1:1000; AB0040-200, SICGEN, Cantanhede, Portugal); chicken anti-dsRed (1:3000; CPCA-mcherry, Encor Biotechnology, Gainesville, FL); goat anti-SOX10 (1:500; AF2864, R&D, Minneapolis, MN); mouse anti-TUJ1 (1:3000; ab78078, Abcam); rat anti–PECAM-1 (1:4000; 553371, BD Pharmingen, San Diego, CA); goat anti-RET (1:500; sc-167-G, Santa Cruz, Dallas, TX); rabbit anti-P75 (1:200; G3231, Promega, Madison, WI); rabbit anti–B-FABP (1:1000; kindly provided by Thomas Müller)[78]; guinea pig anti-ERBB3 (1:1000; kindly provided by Thomas Müller)[80]; rabbit anti-PHOX2B (1:1000; kindly provided by Jean-François Brunet)[80]; goat anti-PHOX2B (1:1000; AF-4940, R&D, Mnneapolis, MN); rabbit anti-PHOX2B (for human samples: 1:250; EPR14423, Abcam, Cambridge, UK); rabbit anti-PH3 (1:1000; 04-817, ThermoFisher); mouse anti-type 1 anti-neuronal nuclear (1:1000; A-21271, ThermoFisher); rabbit anti-glial fibrillary acidic protein (1:1000; Z0334, Dako, Santa Clara, CA); and mouse anti-S100 (1:500; MAB079-1, Millipore, Burlington, MA). The secondary antibodies used were Alexa-405, Alexa-488, Alexa-555, and Alexa-637 (all at 1:1000; Life Technologies, Carlsbad, CA).

Single-Molecule RNA In Situ Hybridization

Gdnf (cat no. 421941-C2, targeting 421-1446 of NM_007903.5) and *Edn3* (cat no. 505841, targeting 12-765 of NM_010275.2) RNAscope probes were designed and manufactured by Advanced Cell Diagnostics (Newark, CA). Serial sections from E14.5 embryos were cut at 20 μm and collected for in situ hybridization following the protocols provided by the manufacturer.[81]

Microscopy and Imaging

Images were collected on an Olympus Fluoview FV3000 confocal microscope (Olympus, Beijing, China). Whole-embryo and gut images were obtained by tile scanning with a 10× objective and automatic stitching. Images were processed and analyzed with Adobe Photoshop (Adobe, San Jose, CA) and ImageJ (version 1.53g; National Institutes of Health, Bethesda, MD).

Statistical Analyses

Based on the assumptions of normality, the Kruskal–Wallis test and *t* test were used to perform statistical analyses with the aid of GraphPad Prism Software v7.0 (GraphPad; San Diego, CA). Results are expressed as means ± SEM. Statistical significance was assumed if the *P* value was less than .05. For each experimental group, at least 3 embryonic samples from at least 2 pregnant mice were analyzed. Detailed statistical information for n and *P* values for each experiment are listed in the corresponding figure legends.

References

1. Yntema CL, Hammond WS. The origin of intrinsic ganglia of trunk viscera from vagal neural crest in the chick embryo. J Comp Neurol 1954;101:515–541.
2. Le Douarin NM, Teillet MA. The migration of neural crest cells to the wall of the digestive tract in avian embryo. J Embryol Exp Morphol 1973;30:31–48.
3. Obermayr F, Hotta R, Enomoto H, Young HM. Development and developmental disorders of the enteric nervous system. Nat Rev Gastroenterol Hepatol 2013; 10:43–57.
4. Heuckeroth RO. Hirschsprung disease - integrating basic science and clinical medicine to improve outcomes. Nat Rev Gastroenterol Hepatol 2018;15:152–167.
5. O'Donnell AM, Puri P. Skip segment Hirschsprung's disease: a systematic review. Pediatr Surg Int 2010; 26:1065–1069.
6. Friedmacher F, Puri P. Rectal suction biopsy for the diagnosis of Hirschsprung's disease: a systematic review of diagnostic accuracy and complications. Pediatr Surg Int 2015;31:821–830.
7. Coe A, Avansino JR, Kapur RP. Distal rectal skip-segment Hirschsprung disease and the potential for false-negative diagnosis. Pediatr Dev Pathol 2016; 19:123–131.
8. Keefer GP, Mokrohisky JF. Congenital megacolon (Hirschsprung's disease). Radiology 1954;63:157–175.

9. Sprinz H, Cohen A, Heaton LD. Hirschsprung's disease with skip area. Ann Surg 1961;153:143–148.

10. MacIver AG, Whitehead R. Zonal colonic aganglionosis, a variant of Hirschsprung's disease. Arch Dis Child 1972; 47:233–237.

11. Martin LW, Buchino JJ, LeCoultre C, Ballard ET, Neblett WW. Hirschsprung's disease with skip area (segmental aganglionosis). J Pediatr Surg 1979; 14:686–687.

12. de Chadarevian JP, Slim M, Akel S. Double zonal aganglionosis in long segment Hirschsprung's disease with a "skip area" in transverse colon. J Pediatr Surg 1982;17:195–197.

13. Yunis E, Sieber WK, Akers DR. Does zonal aganglionosis really exist? Report of a rare variety of Hirschsprung's disease and review of the literature. Pediatr Pathol 1983; 1:33–49.

14. Taguchi T, Tanaka K, Ikeda K, Hata A. Double zonal aganglionosis with a skipped oligoganglionic ascending colon. Z Kinderchir 1983;38:312–315.

15. Seldenrijk CA, van der Harten HJ, Kluck P, Tibboel D, Moorman-Voestermans K, Meijer CJ. Zonal aganglionosis. An enzyme and immunohistochemical study of two cases. Virchows Arch A Pathol Anat Histopathol 1986;410:75–81.

16. Anderson KD, Chandra R. Segmental aganglionosis of the appendix. J Pediatr Surg 1986;21:852–854.

17. Kapur RP, deSa DJ, Luquette M, Jaffe R. Hypothesis: pathogenesis of skip areas in long-segment Hirschsprung's disease. Pediatr Pathol Lab Med 1995; 15:23–37.

18. Yang HY, Liu QL, Wang JX, Xu HF. [Clinical study of multiple zonal aganglionosis in long segment Hirschsprung's disease]. Zhonghua Yi Xue Za Zhi 2005; 85:2772–2774.

19. Ziad F, Katchy KC, Al Ramadan S, Alexander S, Kumar S. Clinicopathological features in 102 cases of Hirschsprung disease. Ann Saudi Med 2006; 26:200–204.

20. Oshio T. Imperforate anus, malrotation, and Hirschsprung's disease with double zonal aganglionosis: an extremely rare combination. J Pediatr Surg 2008; 43:222–226.

21. O'Donnell AM, Puri P. Skip segment Hirschsprung's disease: a rare phenomenon. European Union Paediatric Surgery Association 2010 Meeting 2010; Berne, Switzerland.

22. Doi T, O'Donnell AM, McDermott M, Puri P. Skip segment Hirschsprung's disease: a rare phenomenon. Pediatr Surg Int 2011;27:787–789.

23. Burjonrappa S, Rankin L. 'Hop the skip' with extended segment intestinal biopsy in Hirschsprung's disease. Int J Surg Case Rep 2012;3:186–189.

24. Moore SW, Sidler D, Schubert PA. Segmental aganglionosis (zonal aganglionosis or "skip" lesions) in Hirschsprungs disease: a report of 2 unusual cases. Pediatr Surg Int 2013;29:495–500.

25. Erten EE, Cavusoglu YH, Arda N, Karaman A, Afsarlar CE, Karaman I, Ozguner IF. A rare case of multiple skip segment Hirschsprung's disease in the ileum and colon. Pediatr Surg Int 2014;30:349–351.

26. Raghunath BV, Shankar G, Babu MN, Kini U, Ramesh S, Jadhav V, Aravind KL. Skip segment Hirschsprung's disease: a case report and novel management technique. Pediatr Surg Int 2014;30:119–122.

27. Gross ER, Geddes GC, McCarrier JA, Jarzembowski JA, Arca MJ. Skip segment Hirschsprung disease and Waardenburg syndrome. J Pediatr Surg Case Rep 2015; 3:143–145.

28. Ruiz SL, Hurtado CM, Fernandes RC, Ossorio JIS, Nunez RN. Skip segment Hirschsprung's disease in a patient with Shah-Waardenburg Syndrome. J Pediatr Surg Case Rep 2016;15:44–47.

29. Alfawaz ARC, Rao K, Sola J, Neville H. Skip segment Hirschsprungs disease: avoiding the potential pitfall of a failed pull-through procedure. EC Paediatrics Special Issue 2017;4:25–28.

30. Shenoy A, De Los Santos Y, Johnson KN, Petroze R. Distal rectal skip segment Hirschsprung disease: case report and review of literature. Fetal Pediatr Pathol 2019; 38:437–443.

31. Burns AJ, Douarin NM. The sacral neural crest contributes neurons and glia to the post-umbilical gut: spatiotemporal analysis of the development of the enteric nervous system. Development 1998; 125:4335–4347.

32. Wang X, Chan AK, Sham MH, Burns AJ, Chan WY. Analysis of the sacral neural crest cell contribution to the hindgut enteric nervous system in the mouse embryo. Gastroenterology 2011;141: 992–1002 e1–6.

33. Coventry S, Yost C, Palmiter RD, Kapur RP. Migration of ganglion cell precursors in the ileoceca of normal and lethal spotted embryos, a murine model for Hirschsprung disease. Lab Invest 1994;71:82–93.

34. Druckenbrod NR, Epstein ML. The pattern of neural crest advance in the cecum and colon. Dev Biol 2005; 287:125–133.

35. Nishiyama C, Uesaka T, Manabe T, Yonekura Y, Nagasawa T, Newgreen DF, Young HM, Enomoto H. Trans-mesenteric neural crest cells are the principal source of the colonic enteric nervous system. Nat Neurosci 2012;15:1211–1218.

36. Takahashi Y, Sipp D, Enomoto H. Tissue interactions in neural crest cell development and disease. Science 2013;341:860–863.

37. Uesaka T, Nagashimada M, Enomoto H. Neuronal differentiation in Schwann cell lineage underlies postnatal neurogenesis in the enteric nervous system. J Neurosci 2015;35:9879–9888.

38. Green SA, Uy BR, Bronner ME. Ancient evolutionary origin of vertebrate enteric neurons from trunk-derived neural crest. Nature 2017;544:88–91.

39. Jessen KR, Mirsky R. The origin and development of glial cells in peripheral nerves. Nat Rev Neurosci 2005; 6:671–682.

40. Watanabe Y, Ito T, Harada T, Kobayashi S, Ozaki T, Nimura Y. Spatial distribution and pattern of extrinsic

nerve strands in the aganglionic segment of congenital aganglionosis: stereoscopic analysis in spotting lethal rats. J Pediatr Surg 1995;30:1471–1476.

41. McCallion AS, Stames E, Conlon RA, Chakravarti A. Phenotype variation in two-locus mouse models of Hirschsprung disease: tissue-specific interaction between Ret and Ednrb. Proc Natl Acad Sci U S A 2003; 100:1826–1831.

42. Coffey JC, O'Leary DP. The mesentery: structure, function, and role in disease. Lancet Gastroenterol Hepatol 2016;1:238–247.

43. Lee HO, Levorse JM, Shin MK. The endothelin receptor-B is required for the migration of neural crest-derived melanocyte and enteric neuron precursors. Dev Biol 2003;259:162–175.

44. Plummer NW, Evsyukova IY, Robertson SD, de Marchena J, Tucker CJ, Jensen P. Expanding the power of recombinase-based labeling to uncover cellular diversity. Development 2015;142:4385–4393.

45. Hirsch MR, d'Autreaux F, Dymecki SM, Brunet JF, Goridis C. A Phox2b::FLPo transgenic mouse line suitable for intersectional genetics. Genesis 2013; 51:506–514.

46. Young HM, Newgreen D. Enteric neural crest-derived cells: origin, identification, migration, and differentiation. Anat Rec 2001;262:1–15.

47. Young HM, Hearn CJ, Ciampoli D, Southwell BR, Brunet JF, Newgreen DF. A single rostrocaudal colonization of the rodent intestine by enteric neuron precursors is revealed by the expression of Phox2b, Ret, and p75 and by explants grown under the kidney capsule or in organ culture. Dev Biol 1998;202:67–84.

48. Espinosa-Medina I, Jevans B, Boismoreau F, Chettouh Z, Enomoto H, Muller T, Birchmeier C, Burns AJ, Brunet JF. Dual origin of enteric neurons in vagal Schwann cell precursors and the sympathetic neural crest. Proc Natl Acad Sci U S A 2017;114:11980–11985.

49. Niu X, Liu L, Wang T, Chuan X, Yu Q, Du M, Gu Y, Wang L. Mapping of extrinsic innervation of the gastrointestinal tract in the mouse embryo. J Neurosci 2020; 40:6691–6708.

50. Hosoda K, Hammer RE, Richardson JA, Baynash AG, Cheung JC, Giaid A, Yanagisawa M. Targeted and natural (piebald-lethal) mutations of endothelin-B receptor gene produce megacolon associated with spotted coat color in mice. Cell 1994;79:1267–1276.

51. Young HM, Jones BR, McKeown SJ. The projections of early enteric neurons are influenced by the direction of neural crest cell migration. J Neurosci 2002; 22:6005–6018.

52. Debbache J, Parfejevs V, Sommer L. Cre-driver lines used for genetic fate mapping of neural crest cells in the mouse: an overview. Genesis 2018;56:e23105.

53. Kaukua N, Shahidi MK, Konstantinidou C, Dyachuk V, Kaucka M, Furlan A, An Z, Wang L, Hultman I, Ahrlund-Richter L, Blom H, Brismar H, Lopes NA, Pachnis V, Suter U, Clevers H, Thesleff I, Sharpe P, Ernfors P, Fried K, Adameyko I. Glial origin of mesenchymal stem cells in a tooth model system. Nature 2014; 513:551–554.

54. Hao MM, Bornstein JC, Young HM. Development of myenteric cholinergic neurons in ChAT-Cre;R26R-YFP mice. J Comp Neurol 2013;521:3358–3370.

55. Bialkowska AB, Ghaleb AM, Nandan MO, Yang VW. Improved Swiss-rolling technique for intestinal tissue preparation for immunohistochemical and immunofluorescent analyses. J Vis Exp 2016;113:54161.

56. Skinner MA, Kalyanaraman S, Safford SD, Heuckeroth RO, Tourtellotte W, Goyeau D, Goodfellow P, Milbrandt JD, Freemerman A. A human yeast artificial chromosome containing the multiple endocrine neoplasia type 2B Ret mutation does not induce medullary thyroid carcinoma but does support the growth of kidneys and partially rescues enteric nervous system development in Ret-deficient mice. Am J Pathol 2005;166:265–274.

57. Baynash AG, Hosoda K, Giaid A, Richardson JA, Emoto N, Hammer RE, Yanagisawa M. Interaction of endothelin-3 with endothelin-B receptor is essential for development of epidermal melanocytes and enteric neurons. Cell 1994;79:1277–1285.

58. Ikeya M, Lee SM, Johnson JE, McMahon AP, Takada S. Wnt signalling required for expansion of neural crest and CNS progenitors. Nature 1997;389:966–970.

59. Dunn KJ, Williams BO, Li Y, Pavan WJ. Neural crest-directed gene transfer demonstrates Wnt1 role in melanocyte expansion and differentiation during mouse development. Proc Natl Acad Sci U S A 2000; 97:10050–10055.

60. Lewis AE, Vasudevan HN, O'Neill AK, Soriano P, Bush JO. The widely used Wnt1-Cre transgene causes developmental phenotypes by ectopic activation of Wnt signaling. Dev Biol 2013;379:229–234.

61. Edery P, Lyonnet S, Mulligan LM, Pelet A, Dow E, Abel L, Holder S, Nihoul-Fekete C, Ponder BA, Munnich A. Mutations of the RET proto-oncogene in Hirschsprung's disease. Nature 1994;367:378–380.

62. Schuchardt A, D'Agati V, Larsson-Blomberg L, Costantini F, Pachnis V. Defects in the kidney and enteric nervous system of mice lacking the tyrosine kinase receptor Ret. Nature 1994;367:380–383.

63. Bondurand N, Natarajan D, Barlow A, Thapar N, Pachnis V. Maintenance of mammalian enteric nervous system progenitors by SOX10 and endothelin 3 signalling. Development 2006;133:2075–2086.

64. Bondurand N, Dufour S, Pingault V. News from the endothelin-3/EDNRB signaling pathway: role during enteric nervous system development and involvement in neural crest-associated disorders. Dev Biol 2018;444-(Suppl 1):S156–S169.

65. Young HM, Hearn CJ, Farlie PG, Canty AJ, Thomas PQ, Newgreen DF. GDNF is a chemoattractant for enteric neural cells. Dev Biol 2001;229:503–516.

66. Natarajan D, Marcos-Gutierrez C, Pachnis V, de Graaff E. Requirement of signalling by receptor tyrosine kinase RET for the directed migration of enteric nervous system progenitor cells during mammalian embryogenesis. Development 2002;129:5151–5160.

67. Leibl MA, Ota T, Woodward MN, Kenny SE, Lloyd DA, Vaillant CR, Edgar DH. Expression of endothelin 3 by

mesenchymal cells of embryonic mouse caecum. Gut 1999;44:246–252.

68. Shin MK, Levorse JM, Ingram RS, Tilghman SM. The temporal requirement for endothelin receptor-B signalling during neural crest development. Nature 1999;402:496–501.

69. Burns AJ, Champeval D, Le Douarin NM. Sacral neural crest cells colonise aganglionic hindgut in vivo but fail to compensate for lack of enteric ganglia. Dev Biol 2000;219:30–43.

70. Newgreen DF, Osborne JM, Zhang D. Skip segment Hirschsprung disease: modelling the trans-mesenteric origin of the enteric nervous system in the human colon. bioRxiv 2019;1–24.

71. Fu CG, Muto T, Masaki T, Nagawa H. Zonal adult Hirschsprung's disease. Gut 1996;39:765–767.

72. Uesaka T, Jain S, Yonemura S, Uchiyama Y, Milbrandt J, Enomoto H. Conditional ablation of GFR alpha 1 in postmigratory enteric neurons triggers unconventional neuronal death in the colon and causes a Hirschsprung's disease phenotype. Development 2007;134:2171–2181.

73. Hofstra RM, Wu Y, Stulp RP, Elfferich P, Osinga J, Maas SM, Siderius L, Brooks AS, vd Ende JJ, Heydendael VM, Severijnen RS, Bax KM, Meijers C, Buys CH. RET and GDNF gene scanning in Hirschsprung patients using two dual denaturing gel systems. Hum Mutat 2000;15:418–429.

74. Chakravarti A. Endothelin receptor-mediated signaling in Hirschsprung disease. Hum Mol Genet 1996; 5:303–307.

75. Tang CS, Li P, Lai FP, Fu AX, Lau ST, So MT, Lui KN, Li Z, Zhuang X, Yu M, Liu X, Ngo ND, Miao X, Zhang X, Yi B, Tang S, Sun X, Zhang F, Liu H, Liu Q, Zhang R, Wang H, Huang L, Dong X, Tou J, Cheah KS, Yang W, Yuan Z, Yip KY, Sham PC, Tam PK, Garcia-Barcelo MM, Ngan ES. Identification of genes associated with Hirschsprung disease, based on whole-genome sequence analysis, and potential effects on enteric nervous system development. Gastroenterology 2018; 155:1908–1922 e5.

76. Parlato R, Otto C, Begus Y, Stotz S, Schutz G. Specific ablation of the transcription factor CREB in sympathetic neurons surprisingly protects against developmentally regulated apoptosis. Development 2007; 134:1663–1670.

77. Wang L, Klein R, Zheng B, Marquardt T. Anatomical coupling of sensory and motor nerve trajectory via axon tracking. Neuron 2011;71:263–277.

78. Grossmann KS, Wende H, Paul FE, Cheret C, Garratt AN, Zurborg S, Feinberg K, Besser D, Schulz H, Peles E, Selbach M, Birchmeier W, Birchmeier C. The tyrosine phosphatase Shp2 (PTPN11) directs neuregulin-1/ErbB signaling throughout Schwann cell development. Proc Natl Acad Sci U S A 2009;106:16704–16709.

79. Sheean ME, McShane E, Cheret C, Walcher J, Muller T, Wulf-Goldenberg A, Hoelper S, Garratt AN, Kruger M, Rajewsky K, Meijer D, Birchmeier W, Lewin GR, Selbach M, Birchmeier C. Activation of MAPK overrides the termination of myelin growth and replaces Nrg1/ErbB3 signals during Schwann cell development and myelination. Gene Dev 2014;28:290–303.

80. Pattyn A, Morin X, Cremer H, Goridis C, Brunet JF. Expression and interactions of the two closely related homeobox genes Phox2a and Phox2b during neurogenesis. Development 1997;124:4065–4075.

81. Wang F, Flanagan J, Su N, Wang LC, Bui S, Nielson A, Wu XY, Vo HT, Ma XJ, Luo YL. RNAscope a novel in situ RNA analysis platform for formalin-fixed, paraffin-embedded tissues. J Mol Diagn 2012;14:22–29.

Correspondence
Address correspondence to: Liang Wang, PhD, Institute of Neuroscience, Zhejiang University School of Medicine, 866 Yu Hang Tang Road, Hangzhou 310058, China. e-mail: lwang1@zju.edu.cn; fax: (86) 571-88981757.